

# Nonperturbative resummation of de Sitter infrared logarithms in the large- $N$ limit

J. Serreau\*

*Astro-Particule et Cosmologie (APC), CNRS UMR 7164, Université Paris 7 - Denis Diderot  
10, rue Alice Domon et Léonie Duquet, 75205 Paris Cedex 13, France*

R. Parentani†

*Laboratoire de Physique Théorique (LPT), CNRS UMR 8627,  
Bât. 210, Université Paris - Sud 11, 91405 Orsay Cedex, France*

(Dated: July 13, 2018)

We study the  $O(N)$  scalar field theory with quartic self-coupling in de Sitter space. When the field is light in units of the expansion rate, perturbative methods break down at very low momenta due to large infrared logarithmic terms. Using the nonperturbative large- $N$  limit, we compute the four-point vertex function in the deep infrared regime. The resummation of an infinite series of perturbative (bubble) diagrams leads to a modified power law which is analogous to the generation of an anomalous dimension in critical phenomena. We discuss in detail the role of high momentum (subhorizon) modes, including the issue of renormalization, and show that they influence the dynamics of infrared (superhorizon) modes only through a constant renormalization factor. This provides an explicit example of effective decoupling between high and low energy physics in an expanding space-time.

PACS numbers: 11.10.-z, 04.62.+v

Keywords: Quantum field theory, de Sitter space, large- $N$  techniques

## I. INTRODUCTION

The study of quantum field dynamics on de Sitter space has received strong phenomenological motivations with the impressive observational success of the inflation paradigm and the need to compute quantum corrections to inflationary observables and with the observation of the recent acceleration of the Universe. Radiative corrections on de Sitter space have been addressed in a variety of field theories, mainly based on perturbative loop expansion [1–7]. In the phenomenologically relevant case of a light field, with a mass small as compared to the Hubble parameter, loop diagrams typically exhibit large infrared (IR) logarithms, unless they are protected by some symmetries [8–11]. In addition, in cases where the de Sitter symmetry is broken, e.g., by finite time initial conditions, loop corrections give secular divergences which grow as powers of the number of e-folds [4, 11–15]. The understanding of such IR/secular divergences is of key importance for a fundamental description of quantum field dynamics in de Sitter space. For instance, it is unknown whether they signal an instability of de Sitter space against quantum fluctuations [16–22]. In any case, such divergences pose a problem of principle and call for resummation.

The situation is somewhat similar to the appearance of large logarithms in standard quantum field theory (QFT). These signals a breakdown of perturbation the-

ory and their resummation lead to nontrivial phenomena such as running couplings or anomalous scaling of field correlators [23, 24]. IR and/or secular divergences are common features of perturbative approaches e.g. for bosonic theories at high temperatures [25] or near a second order phase transition [24] or in the case of nonequilibrium systems [26]. Various resummation techniques or nonperturbative approaches have been developed over the years to cope with such issues in flat space-time. These include, e.g., large- $N$  techniques [27, 28], the renormalization group [24, 29], hard thermal loops [25], or two-particle-irreducible (2PI) techniques [26, 30]. Recently, some effort has been put in trying to extend these techniques to the case of IR/secular divergences in de Sitter space [15, 31–41].

The large- $N$  limit in  $O(N)$  scalar theories provides a simple nonperturbative approach which captures nontrivial IR physics in flat space-time [27, 28, 42–44]. Recently this approach has been applied in de Sitter space with interesting results [31, 33]. For instance, it describes dynamical mass generation, first pointed out in [12], which screens perturbative IR divergences and renders the theory well behaved. The generated mass exhibits a nonanalytic dependence in the coupling, which is typical of nonperturbative IR physics. Also it has been shown that strong IR fluctuations prohibit the possibility of a spontaneously broken phase [33, 45], a phenomenon akin to what happens in two-dimensional flat space-time [46].

The phenomena described here involve the resummation of a particular class of IR divergences corresponding to purely local contributions to the self-energy. Such masslike contributions are specific to theories with quar-

---

\*Electronic address: serreau@apc.univ-paris7.fr

†Electronic address: parentani@th.u-psud.fr

tic self-interactions and are technically easy to deal with due to their local character. Less simple but more generic are the logarithmic IR divergencies arising from nonlocal perturbative diagrams.

In the present paper we consider the four-point vertex function of an  $O(N)$  scalar field theory. In the large- $N$  limit, the latter is given by an infinite series of nonlocal bubble loop diagrams, each of which bringing additional IR logarithms. Exploiting the physical momentum space representation (hereafter called  $p$ -representation) for de Sitter correlators [39, 47, 48], we show that this series can be exactly resummed. This induces a modification of the IR power law behavior in a similar way as the resummation of large logarithms in standard QFT, e.g., at a critical point, produces an anomalous scaling of field correlators.

The nonlocal character of the physics described above leads to a nontrivial interplay between IR and ultraviolet (UV) momentum modes. In the main body of the paper, we simply disregard high-momentum modes. This allows us to exhibit the anomalous dimension phenomenon in arbitrary dimension. We show that the results are essentially insensitive to the scale which separates IR and UV modes. A detailed analysis of the role of UV modes in four space-time dimension—including a discussion of renormalization—is presented in the Appendices together with some technical material needed for the main body of the paper. Remarkably, we find that UV modes do not alter the IR power law behaviors and merely give rise to a finite computable constant renormalization factor. This demonstrates a form of effective decoupling between IR and UV physics in de Sitter.

In Sec. II we briefly review the main aspects of the  $p$ -representation of de Sitter correlators. Then Sec. III focuses on the  $O(N)$  scalar theory in the large- $N$  limit for both the two- and the four-point vertex functions. We recall the solution of the corresponding equations for the two-point function, which describes self-consistent mass generation in Sec. IV. The analysis of the four-point function and the resummation of nonlocal IR logarithms is performed in Sec. V, where we neglect UV modes. The important technical details needed for this analysis are presented in Appendices A-C. Finally, Appendices D-G present a detailed treatment of UV modes in four space-time dimensions, where the present theory is perturbatively renormalizable.

## II. $p$ -REPRESENTATION OF TWO-POINT CORRELATORS IN DE SITTER SPACE

We consider a generic quantum scalar field  $\varphi(x)$  on the expanding Poincaré patch of de Sitter space-time with  $D = d + 1$  dimensions and expansion rate  $H = 1$ . The line element is given by

$$ds^2 = a^2(\eta) (-d\eta^2 + d\mathbf{X}^2)$$

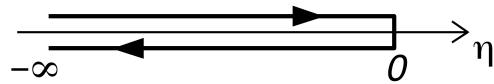


FIG. 1: The closed path  $\mathcal{C} = \mathcal{C}^+ \cup \mathcal{C}^-$  in conformal time  $\eta$ . The forward (upper) branch  $\mathcal{C}^+$  goes from  $-\infty$  to  $0^-$  and the backward (lower) branch  $\mathcal{C}^-$  goes back from  $0^-$  to  $-\infty$ .

in terms of the conformal time  $\eta$  and comoving spatial coordinates  $\mathbf{X}$ , with  $a(\eta) = -1/\eta = e^t$  with  $t \in \mathbb{R}$ .

Like general nonequilibrium quantum systems [26, 49–52], quantum field theories in cosmological spaces can be conveniently formulated using a closed contour  $\mathcal{C}$  in the time coordinate [39, 53, 54]. The appropriate contour for conformal time is depicted in Fig. 1. The various components of  $n$ -point correlators are then described by means of time ordered products of field operators on the contour. For instance the two-point function  $G(x, x') = \langle T_{\mathcal{C}} \varphi(x) \varphi(x') \rangle$ , where  $T_{\mathcal{C}}$  denotes time ordering on the contour  $\mathcal{C}$ , encodes both the statistical and spectral correlators<sup>1</sup>  $F(x, x') = \frac{1}{2} \langle \{ \varphi(x), \varphi(x') \} \rangle$  and  $\rho(x, x') = i \langle [ \varphi(x), \varphi(x') ] \rangle$ :

$$G(x, x') = F(x, x') - \frac{i}{2} \text{sign}_{\mathcal{C}}(x^0 - x'^0) \rho(x, x'), \quad (1)$$

where the sign function is to be understood along the contour  $\mathcal{C}$ . In the rest of this subsection, we consider the statistical function  $F$ . Everything holds equally for the spectral function  $\rho$ .

De Sitter invariance ensures that the two-point function  $F(x, x')$  only depends on the invariant distance  $z(x, x')$ . In the coordinate system (1), the latter reads

$$z(x, x') = \frac{\eta^2 + \eta'^2 - (\mathbf{X} - \mathbf{X}')^2}{2\eta\eta'}. \quad (2)$$

The dependence on comoving spatial variable is only through  $|\mathbf{X} - \mathbf{X}'|$ , which reflects the spatial homogeneity and isotropy of de Sitter space-time in this coordinate system.

It proves convenient to introduce conformally rescaled quantities, such as the rescaled field  $\phi(x) = a^{\frac{d-1}{2}}(\eta) \varphi(x)$  and its correlators. One has, for instance,

$$F(x, x') = [a(\eta)a(\eta')]^{-\frac{d-1}{2}} F_c(\eta, \eta', |\mathbf{X} - \mathbf{X}'|), \quad (3)$$

where  $F_c(\eta, \eta', |\mathbf{X} - \mathbf{X}'|) = \frac{1}{2} \langle \{ \phi(x), \phi(x') \} \rangle$ . Introducing spatial comoving momentum variables, one defines

$$\tilde{F}_c(\eta, \eta', K) = \int d^d S e^{-i\mathbf{K} \cdot \mathbf{S}} F_c(\eta, \eta', |\mathbf{S}|). \quad (4)$$

Spatial homogeneity implies the conservation of the comoving momentum.

<sup>1</sup> We use  $\{A, B\} = AB + BA$  and  $[A, B] = AB - BA$ .



FIG. 2: The closed path  $\hat{\mathcal{C}} = \hat{\mathcal{C}}^+ \cup \hat{\mathcal{C}}^-$  in the momentum variable  $p = -K\eta$ . The upper branch  $\hat{\mathcal{C}}^+$  goes from  $+\infty$  to  $0^+$  and the lower branch  $\hat{\mathcal{C}}^-$  goes back from  $0^+$  to  $+\infty$ .

Specializing to de Sitter, an extra symmetry implies that two-point correlators follow the scaling law [39, 48]

$$\tilde{F}_c(\eta, \eta', K) = \frac{1}{K} \hat{F}(p, p'), \quad (5)$$

where  $p = -K\eta$  and  $p' = -K\eta'$  are the physical momenta at times  $\eta$  and  $\eta'$  respectively. Eq. (5) provides the  $p$ -representation of the two-point correlator.

As mentioned previously Eq. (5) applies to the spectral function  $\rho$  as well. In fact, as in (1), one can combine the statistical and spectral two-point functions in a single propagator defined on a closed contour  $\hat{\mathcal{C}}$  in physical momentum [39]:

$$\hat{G}(p, p') = \hat{F}(p, p') - \frac{i}{2} \text{sign}_{\hat{\mathcal{C}}}(p - p') \hat{\rho}(p, p'). \quad (6)$$

The sign function is to be understood on the contour depicted in Fig. 2. We also note the symmetry properties  $F(p, p') = F(p', p)$  and  $\rho(p, p') = -\rho(p', p)$ .

### III. $O(N)$ SCALAR FIELD THEORY IN THE LARGE- $N$ LIMIT

We consider an  $O(N)$  scalar theory, defined by the classical action

$$\mathcal{S}[\varphi] = \int_x \left\{ \frac{1}{2} \varphi_a (\square - m_{\text{dS}}^2) \varphi_a - \frac{\lambda}{4!N} (\varphi_a \varphi_a)^2 \right\}, \quad (7)$$

where  $a = 1, \dots, N$  and a summation over repeated indices is understood. Here,

$$\square \equiv \frac{1}{\sqrt{-g(x)}} \partial_\mu \sqrt{-g(x)} g^{\mu\nu} \partial_\nu \quad (8)$$

is the covariant Laplace operator and

$$m_{\text{dS}}^2 = m^2 + \xi R = m^2 + d(d+1)\xi \quad (9)$$

is the effective square mass with  $m$  the tree-level mass and  $\xi$  the coupling to the Ricci scalar  $R = d(d+1)$ . Finally,

$$\int_x \equiv \int d^D x \sqrt{-g(x)} = \int_{\mathcal{C}} dx^0 \int d^d x \sqrt{-g(x)}, \quad (10)$$

where the  $x^0$  integral runs along the contour  $\mathcal{C}$ .

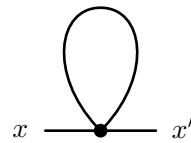


FIG. 3: The self-energy  $\Sigma(x, x')$  in the limit  $N \rightarrow \infty$ . The internal line in the diagram is given by the full propagator  $G(x, x)$ , hence the nonperturbative nature of the large- $N$  limit. This describes self-consistent mass generation.

#### A. The large- $N$ limit

The  $1/N$  expansion provides a controlled expansion scheme which gives access to nonperturbative aspects of the theory. It can be formulated in cosmological spaces [39, 53] using standard functional techniques, provided one employs appropriate covariant quantities such as the functional derivative,

$$\frac{\delta_c}{\delta\varphi(x)} \equiv \frac{1}{\sqrt{-g(x)}} \frac{\delta}{\delta\varphi(x)}, \quad (11)$$

the integration measure (10) and the corresponding covariant Dirac distribution on the contour,

$$\delta^{(D)}(x, x') = \frac{\delta_{\mathcal{C}}(x^0 - x'^0) \delta^{(d)}(\mathbf{x} - \mathbf{x}')}{\sqrt{-g(x)}}, \quad (12)$$

defined such that  $\int_z \delta^{(D)}(x, z) f(z) = f(x)$  for any function  $f$  on the contour. Let us recall the basic equations describing the limit  $N \rightarrow \infty$ , see [39, 43]. It has been shown in [33] that the theory does not admit a de Sitter invariant state with spontaneous symmetry breaking. We thus consider the symmetric phase, where  $\langle \varphi_a \rangle = 0$ ,  $G_{ab} = \delta_{ab} G$  and  $\Sigma_{ab} = \delta_{ab} \Sigma$ . The covariant inverse propagator  $G^{-1}$  is defined as

$$\int_z G^{-1}(x, z) G(z, x') = \delta^{(D)}(x, x'). \quad (13)$$

It can be written in terms of the covariant self-energy as

$$G^{-1}(x, x') = G_0^{-1}(x, x') - \Sigma(x, x'), \quad (14)$$

where

$$iG_0^{-1}(x, x') = (\square_x - m_{\text{dS}}^2) \delta^{(D)}(x, x'). \quad (15)$$

In the large- $N$  limit, the self-energy is given by the tadpole diagram of Fig. 3, where the line represents the propagator  $G$  itself. It thus corresponds to a local, masslike contribution:

$$\Sigma(x, x') = -i\sigma \delta^{(D)}(x, x'), \quad (16)$$

where

$$\sigma = \frac{\lambda}{6} G(x, x). \quad (17)$$

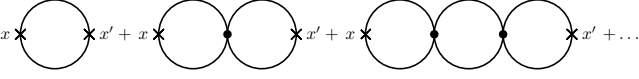


FIG. 4: The infinite series of bubble diagrams contributing to the function  $I(x, x')$ . The black dots denote interaction vertices whereas the crosses are the end points of the function. The elementary one-loop bubble is given by the function  $\Pi(x, x') \propto G^2(x, x')$ . Each addition of a new bubble leads to large IR logarithms in the momentum representation, the infinite series of which resums to a modified power law.

De Sitter symmetry guarantees that the latter is a constant. The propagator  $G$  thus satisfies the equation

$$(\square_x - M^2) G(x, x') = i\delta^{(D)}(x, x'), \quad (18)$$

with a self-consistent square mass

$$M^2 = m_{\text{dS}}^2 + \sigma. \quad (19)$$

The four-point vertex function reads, writing  $x_i \equiv x_1, \dots, x_4$  for brief,

$$\Gamma_{abcd}^{(4)}(x_i) = \delta_{ab}\delta_{cd}\delta^{(D)}(x_1, x_2)\delta^{(D)}(x_3, x_4)iD(x_1, x_3) + \text{perm.}, \quad (20)$$

where “perm.” stands for the two cyclic permutations needed to make  $\Gamma_{abcd}^{(4)}(x_i)$  symmetric. Here, the function

$$iD(x, x') = -\frac{\lambda}{3N} \left[ \delta^{(D)}(x, x') + iI(x, x') \right] \quad (21)$$

is the two-point correlator of the composite field  $\chi = \lambda\varphi_a\varphi_a/6N$ :  $D(x, x') = \langle T_C \chi(x)\chi(x') \rangle$ . The local contribution gives rise to the classical vertex in (20) and the nonlocal one actually corresponds to the infinite sum of bubble diagrams represented in Fig. 4. This infinite sum can be cast into the following integral equation:

$$I(x, x') = \Pi(x, x') + i \int_z \Pi(x, z)I(z, x'), \quad (22)$$

with

$$\Pi(x, x') = -\frac{\lambda}{6} G^2(x, x') \quad (23)$$

the elementary one-loop bubble diagram. The four-point vertex is thus completely expressed in terms of a nontrivial two-point function.

### B. $p$ -representation

The  $p$ -representation plays an important role in the analytical solution presented below. We briefly review the relevant material for our present purposes and refer the reader to Ref. [39] for more details.

Eq. (18) is equivalent to the free-field-like equation for the statistical function  $\hat{F}$  defined in Eqs. (3)-(5)

$$\left[ \partial_p^2 + 1 - \frac{\nu^2 - \frac{1}{4}}{p^2} \right] \hat{F}(p, p') = 0, \quad (24)$$

where

$$\nu = \sqrt{\frac{d^2}{4} - M^2}. \quad (25)$$

The spectral function  $\hat{\rho}(p, p')$  satisfies the same equation. The “initial” data is to be specified at  $p = p' \rightarrow \infty$ . Commutation relations imply  $\hat{\rho}(p, p')|_{p=p'} = \partial_p \partial_{p'} \hat{\rho}(p, p')|_{p=p'} = 0$  and  $\partial_p \hat{\rho}(p, p')|_{p=p'} = -1$  for the spectral function. The statistical function contains the information about the (quantum) state of the system. The only choice compatible with de Sitter symmetry and with the requirement of renormalizability is the Bunch-Davies vacuum [55]. This corresponds to the choice

$$\begin{aligned} \hat{F}(p, p') \Big|_{p=p' \rightarrow \infty} &= \frac{1}{2}, \\ \partial_p \hat{F}(p, p') \Big|_{p=p' \rightarrow \infty} &= 0, \\ \partial_p \partial_{p'} \hat{F}(p, p') \Big|_{p=p' \rightarrow \infty} &= \frac{1}{2}. \end{aligned} \quad (26)$$

With this choice, the solutions of Eq. (24) for  $\hat{F}$  and  $\hat{\rho}$  read

$$\hat{F}(p, p') = \frac{\pi}{4} \sqrt{pp'} \text{Re} \{ H_\nu(p) H_\nu^*(p') \} \quad (27)$$

$$\hat{\rho}(p, p') = -\frac{\pi}{2} \sqrt{pp'} \text{Im} \{ H_\nu(p) H_\nu^*(p') \}, \quad (28)$$

where  $H_\nu(x)$  is the Hankel function of the first kind [56]. Finally, the self-energy (17) reads

$$\sigma = \frac{\lambda}{6} \int_{\mathbf{q}} \frac{\hat{F}(q, q)}{q} = \frac{\lambda\pi}{24} \int_{\mathbf{q}} |H_\nu(q)|^2, \quad (29)$$

where  $\int_{\mathbf{q}} = \int \frac{d^d q}{(2\pi)^d}$ . The self-consistent mass  $M$  is the solution of the gap equation (19) with (29) and (25). For instance, in the case of vanishing or negative tree-level (classical) mass  $m_{\text{dS}}^2 \leq 0$ , where perturbation theory is ill-defined, Eq. (19) describes the dynamical generation of a strictly positive square mass which cures the IR divergences of perturbation theory.

Let us now consider the four-point vertex function (20). Introducing the appropriate conformal factors

$$\Gamma_{abcd}^{(4)}(x_i) = [a(\eta_1) \cdots a(\eta_4)]^{-\frac{d+3}{2}} \Gamma_{c,abcd}^{(4)}(x_i) \quad (30)$$

and going to spatial comoving momentum space, we have, extracting a factor  $(2\pi)^d \delta^{(d)} \left( \sum_{i=1}^4 \mathbf{K}_i \right)$ ,

$$\begin{aligned} \tilde{\Gamma}_{c,abcd}^{(4)}(\eta_i, \mathbf{K}_i) &= [a(\eta_1) \cdots a(\eta_4)]^{\frac{3-d}{4}} \\ &\times \left\{ \delta_{ab}\delta_{cd} \delta_C(\eta_1 - \eta_2) \delta_C(\eta_3 - \eta_4) i\tilde{D}_c(\eta_1, \eta_3, K_{12}) + \text{perm.} \right\}, \end{aligned} \quad (31)$$

where  $K_{ij} = |\mathbf{K}_i + \mathbf{K}_j|$ . Here,  $\tilde{D}_c$  is the comoving momentum representation of the function  $D$ , Eq. (21), defined as

$$D(x, x') = [a(\eta)a(\eta')]^{-\frac{d+1}{2}} D_c(\eta, \eta', |\mathbf{X} - \mathbf{X}'|) \quad (32)$$

and

$$\tilde{D}_c(\eta, \eta', K) = \int d^d S e^{-i\mathbf{K}\cdot\mathbf{S}} D_c(\eta, \eta', |\mathbf{S}|). \quad (33)$$

We define the comoving momentum representations  $\tilde{I}_c$  and  $\tilde{\Pi}_c$  of the functions  $I$  and  $\Pi$ , Eqs. (22) and (23), in the same way as for  $\tilde{D}_c$ . Equation (21) then reads

$$i\tilde{D}_c(\eta, \eta', K) = -\frac{\lambda}{3N} \left[ \delta_C(\eta - \eta') + i\tilde{I}_c(\eta, \eta', K) \right]. \quad (34)$$

As already emphasized, the function  $\tilde{I}_c$  encodes the non-trivial (loop) contribution to the four-point vertex in the large- $N$  limit. It corresponds to the infinite sum of bubble diagrams depicted in Fig. 4 with the elementary one-loop bubble  $\tilde{\Pi}_c$ . The functions  $\tilde{D}_c$  and  $\tilde{\Pi}_c$  and  $\tilde{I}_c$  admit the following  $p$ -representation:

$$\tilde{D}_c(\eta, \eta', K) = K\hat{D}(p, p') \quad (35)$$

and similarly for  $\tilde{\Pi}_c$  and  $\tilde{I}_c$ , where  $p = -K\eta$  and  $p' = -K\eta'$ . Introducing the Dirac distribution on the momentum contour<sup>2</sup>  $\hat{C}$

$$\delta_C(\eta - \eta') = -K\delta_{\hat{C}}(p - p'), \quad (36)$$

one has

$$i\hat{D}(p, p') = -\frac{\lambda}{3N} \left[ -\delta_{\hat{C}}(p - p') + i\hat{I}(p, p') \right]. \quad (37)$$

The one-loop bubble  $\hat{\Pi}$  is given by

$$\hat{\Pi}(p, p') = -\frac{\lambda}{6} (pp')^{\frac{d-3}{2}} \int_{\mathbf{q}} \frac{\hat{G}(qp, qp')}{q} \frac{\hat{G}(rp, rp')}{r}, \quad (38)$$

where  $r = |\mathbf{e} + \mathbf{q}|$ , with  $\mathbf{e}$  an arbitrary unit vector, and the function  $\hat{I}$  solves the following integral equation on the contour  $\hat{C}$ :

$$\hat{I}(p, p') = \hat{\Pi}(p, p') - i \int_{\hat{C}} ds \hat{\Pi}(p, s) \hat{I}(s, p'). \quad (39)$$

Finally, we write the above equations explicitly in terms of their statistical and spectral components on the contour, defined as<sup>3</sup>

$$\hat{\Pi}(p, p') = \hat{\Pi}_F(p, p') - \frac{i}{2} \text{sign}_{\hat{C}}(p - p') \hat{\Pi}_\rho(p, p'), \quad (40)$$

with  $\Pi_F(p, p') = \Pi_F(p', p)$  and  $\Pi_\rho(p, p') = -\Pi_\rho(p', p)$  and similarly for  $\hat{I}$ . One has

$$\hat{\Pi}_F(p, p') = -\frac{\lambda}{6} (pp')^{\frac{d-3}{2}} \int_{\mathbf{q}} \frac{1}{qr} \left\{ \hat{F}(qp, qp') \hat{F}(rp, rp') - \frac{1}{4} \hat{\rho}(qp, qp') \hat{\rho}(rp, rp') \right\} \quad (41)$$

and

$$\hat{\Pi}_\rho(p, p') = -\frac{\lambda}{3} (pp')^{\frac{d-3}{2}} \int_{\mathbf{q}} \frac{\hat{F}(rp, rp') \hat{\rho}(rp, rp')}{qr}. \quad (42)$$

Writing explicitly the integrals on the contour  $\hat{C}$  in (39), one obtains the following equations

$$\hat{I}_\rho(p, p') = \hat{\Pi}_\rho(p, p') + \int_p^{p'} ds \hat{\Pi}_\rho(p, s) \hat{I}_\rho(s, p') \quad (43)$$

and

$$\hat{I}_F(p, p') = \hat{\Pi}_H(p, p') + \int_p^\infty ds \hat{\Pi}_H(p, s) \hat{I}_F(s, p'), \quad (44)$$

where we introduced the auxiliary function

$$\hat{\Pi}_H(p, p') = \hat{\Pi}_F(p, p') - \int_{p'}^\infty ds \hat{\Pi}_F(p, s) \hat{I}_\rho(s, p'). \quad (45)$$

For later use, we note that, using (43), Eq. (44) can be solved in terms of the function  $\hat{I}_\rho$  as, see Appendix A,

$$\hat{I}_F(p, p') = \hat{\Pi}_H(p, p') + \int_p^\infty ds \hat{I}_\rho(p, s) \hat{\Pi}_H(s, p'). \quad (46)$$

In the next two sections, we solve the above equations in the deep IR limit, that is for  $p, p' \ll 1$  in the case of light fields,  $M^2 \ll 1$ . We adopt the following general strategy: we first assume that the IR physics is dominated by IR modes and we cut all momentum integrals (either in momentum loops or in “time” integrals) at a momentum scale  $\mu \lesssim 1$ . We shall see that we can find a closed solution of the equations in that case and we verify *a posteriori* that the solution weakly depends on the scale  $\mu$ . Of course this is not a proof of our assumption, merely a consistency check. We defer to the Appendices a more complete analysis taking into account the role of high momentum modes. There we show that our results only get slightly modified by a constant renormalization factor. Similarly, we neglect renormalization aspects in the main course of the text and defer their discussion to Appendix G.

#### IV. TWO-POINT FUNCTION: MASS GENERATION

The solution of the gap equation (19) has been discussed in [31–33]. Here, we briefly review the main results and introduce some necessary material for the next section, where we compute the four-point function.

<sup>2</sup> The latter is defined such that  $\int_{\hat{C}} dp' \delta_{\hat{C}}(p - p') \hat{f}(p') = \hat{f}(p)$  for any function  $\hat{f}$  on the contour  $\hat{C}$ . The minus sign in (36) copes for the “wrong” orientation of the momentum contour. Note, in particular, that  $\int_{\hat{C}} dp = -K \int_C d\eta$  [39].

<sup>3</sup> This decomposition is modified by renormalization. However, the final equations to be discussed here are unchanged, see Appendix G.

In the case of light fields, with  $M < d/2$ , the index  $\nu$  is real and  $0 < \nu < d/2$ . It is customary to introduce the parameter  $\varepsilon = d/2 - \nu$ . For small mass, one has  $\varepsilon \approx M^2/d$ . Following the strategy described above, we only need the statistical and spectral correlators  $\hat{F}$  and  $\hat{\rho}$  in the IR regime, i.e., for  $p, p' \ll 1$ . The latter are given by, see Appendix B,

$$\hat{F}_{\text{IR}}(p, p') = \frac{F_\nu}{(pp')^{\nu-\frac{1}{2}}}, \quad (47)$$

where  $F_\nu = [2^\nu \Gamma(\nu)]^2 / 4\pi$  and

$$\hat{\rho}_{\text{IR}}(p, p') = -\frac{\sqrt{pp'}}{2\nu} \left[ \left( \frac{p}{p'} \right)^\nu - \left( \frac{p'}{p} \right)^\nu \right]. \quad (48)$$

It proves useful to rewrite the latter expression as

$$\hat{\rho}_{\text{IR}}(p, p') = -\sqrt{pp'} \mathcal{P}_\nu \left( \ln \frac{p}{p'} \right), \quad (49)$$

with

$$\mathcal{P}_\nu(x) = \frac{\sinh(\nu x)}{\nu}. \quad (50)$$

Restricting the momentum integration in (29) to the IR part  $|\mathbf{q}| < \mu$ , one gets

$$\sigma = \frac{\lambda}{6} \int_{|\mathbf{q}| < \mu} \frac{\hat{F}_{\text{IR}}(q, q)}{q} \approx \frac{\lambda F_\nu}{12\varepsilon} \frac{\Omega_d}{(2\pi)^d}, \quad (51)$$

up to corrections of relative order  $\varepsilon \ln \mu \ll 1$ . Here  $\Omega_d = 2\pi^{d/2} / \Gamma(d/2)$ . Using  $\varepsilon \approx M^2/d$  in the small mass case, it is easy to solve the gap equation (19). For instance, in the case of vanishing tree-level mass,  $m_{\text{dS}}^2 = 0$ , one gets

$$M^2 = \sqrt{\frac{\lambda F_\nu}{12} \frac{d\Omega_d}{(2\pi)^d}} \quad (52)$$

so that

$$\varepsilon = \frac{\sigma}{d} = \frac{\alpha(d/2)}{12\pi} \sqrt{\lambda} \quad (53)$$

where  $\alpha(x) = \sqrt{3\Gamma(x)/x\pi^{x-1}}$  is chosen here so that  $\alpha(3/2) = 1$  for  $d = 3$ . The self-consistent square mass (52) is nonanalytic in the coupling, reflecting its nonperturbative IR character.

## V. FOUR-POINT FUNCTION: RESUMMING INFRARED LOGARITHMS

The first step in the calculation of the four-point vertex is the evaluation of the bubble  $\hat{\Pi}$ , Eqs. (41) and (42). Restricting the loop integral to the contribution from IR modes, i.e. such that  $qp, qp' \lesssim \mu$ , which also implies  $rp, rp' \lesssim \mu$ , one can replace the propagators  $\hat{F}$  and  $\hat{\rho}$  in

Eqs. (41) and (42) by their IR expressions (47)–(50). The loop integrals are performed in Appendix C. We obtain

$$\hat{\Pi}_F^{\text{IR}}(p, p') = \frac{\pi_F}{(pp')^{\kappa+\frac{1}{2}}}, \quad (54)$$

with  $\kappa = \frac{d}{2} - 2\varepsilon$  (notice that  $\kappa = \nu - \varepsilon < \nu$ ) and

$$\hat{\Pi}_\rho^{\text{IR}}(p, p') = \frac{\pi_\rho}{\sqrt{pp'}} \mathcal{P}_\nu^\varepsilon \left( \ln \frac{p}{p'} \right), \quad (55)$$

where we defined the odd function

$$\mathcal{P}_\nu^\varepsilon(x) = e^{-\varepsilon|x|} \mathcal{P}_\nu(x), \quad (56)$$

with  $\mathcal{P}_\nu(x)$  given in (50), and where

$$\pi_\rho = \frac{\lambda F_\nu}{6\varepsilon} \frac{\Omega_d}{(2\pi)^d} = 2\sigma \quad \text{and} \quad \pi_F = -\pi_\rho F_\nu. \quad (57)$$

Let us first consider Eq. (43) for  $\hat{I}_\rho$ . We seek a solution of the form

$$\hat{I}_\rho^{\text{IR}}(p, p') = \frac{\pi_\rho}{\sqrt{pp'}} \mathcal{I}_\varepsilon \left( \ln \frac{p}{p'} \right), \quad (58)$$

where

$$\mathcal{I}_\varepsilon(x) = e^{-\varepsilon|x|} \mathcal{I}(x). \quad (59)$$

with  $\mathcal{I}(x)$  an unknown odd function, as implied by the antisymmetry of  $\hat{I}_\rho(p, p')$  in the exchange  $p \leftrightarrow p'$ . The  $\exp(-\varepsilon|x|)$  terms cancel out in Eq. (43) and we are left with the following integral equation:

$$\mathcal{I}(x) = \mathcal{P}_\nu(x) - \pi_\rho \int_0^x dy \mathcal{P}_\nu(x-y) \mathcal{I}(y). \quad (60)$$

As a first attempt to solve this equation, one may try an expansion in the parameter  $\pi_\rho$  which counts the number of bubbles. This is akin to perturbation theory. At first order, one has

$$\begin{aligned} \mathcal{I}(x) &= \mathcal{P}_\nu(x) - \pi_\rho \int_0^x dy \mathcal{P}_\nu(x-y) \mathcal{P}_\nu(y) + \mathcal{O}(\pi_\rho^2) \\ &= \mathcal{P}_\nu(x) \left( 1 + \frac{\pi_\rho}{2\nu} \left[ 1 - \frac{x}{\tanh(\nu x)} \right] + \mathcal{O}(\pi_\rho^2) \right). \end{aligned} \quad (61)$$

For  $|x| \gg 1$ , that is for large logarithms or, equivalently, large cosmological time separations,  $|\ln(p/p')| = |t - t'| \gg 1$ , we get

$$\mathcal{I}(x) \approx \mathcal{P}_\nu(x) \left( 1 - \frac{\pi_\rho}{2\nu} |x| + \mathcal{O}(\pi_\rho^2) \right). \quad (62)$$

Thus, we see that the true expansion parameter is  $\pi_\rho |x| = \pi_\rho |\ln(p/p')|$  and that the perturbative solution breaks down for  $|\ln(p/p')| = |t - t'| \gtrsim 1/\pi_\rho$ . The argument extends to higher orders and one can check that, in that

case, one has to resum the infinite series of bubble diagrams.

Fortunately, the exact solution of Eq. (60) is easily obtained. It reads

$$\mathcal{I}(x) = \frac{\sinh \bar{\nu} x}{\bar{\nu}} = \mathcal{P}_{\bar{\nu}}(x), \quad (63)$$

where (note that  $\bar{\nu} < \nu$ )

$$\bar{\nu} = \sqrt{\nu^2 - \pi_\rho}. \quad (64)$$

We thus have

$$\hat{I}_\rho^{\text{IR}}(p, p') = \frac{\pi_\rho}{\sqrt{pp'}} \mathcal{P}_{\bar{\nu}}^\varepsilon \left( \ln \frac{p}{p'} \right). \quad (65)$$

We see that resumming the infinite series of bubble diagrams—each producing higher powers of  $\pi_\rho |\ln p/p'|$ —through the integral equation (43) changes the exponent  $\nu$  characterizing the IR power law behavior of the single bubble function  $\hat{\Pi}_\rho$ , see Eq. (55), into the new exponent (64).

Let us now consider the case of  $\hat{I}_F$ , Eq. (44), where, following the general strategy described previously, we replace the upper bound of momentum integrals in (44)–(46) by  $\mu \lesssim 1$ . The contribution of higher momenta is analyzed in Appendix F. We first note that the  $F$  component of the symmetric bubble function  $\hat{\Pi}$  can be written as the following factorized form

$$\hat{\Pi}_F^{\text{IR}}(p, p') = \frac{\pi_F}{\sqrt{pp'}} \mathcal{A} \left( \ln \frac{p}{\mu} \right) \mathcal{A} \left( \ln \frac{p'}{\mu} \right), \quad (66)$$

where we artificially introduced a dependence on  $\mu$  for later convenience. Here,

$$\mathcal{A}(x) = \frac{e^{-\kappa x}}{\mu^\kappa}. \quad (67)$$

The factorization property (66) together with the fact that Eq. (45) for  $\hat{\Pi}_H^{\text{IR}}(p, p')$  only involves the function  $\hat{\Pi}_F^{\text{IR}}(p, s)$  with fixed first argument imply that the auxiliary function takes the asymmetric factorized form,

$$\hat{\Pi}_H^{\text{IR}}(p, p') = \frac{\pi_F}{\sqrt{pp'}} \mathcal{A} \left( \ln \frac{p}{\mu} \right) \bar{\mathcal{A}} \left( \ln \frac{p'}{\mu} \right), \quad (68)$$

with the function  $\mathcal{A}$  given in (67) above and the function  $\bar{\mathcal{A}}$  is to be determined. Using (45) and (58), we find (here  $x = \ln p/\mu < 0$ )

$$\bar{\mathcal{A}}(x) = \mathcal{A}(x) + \pi_\rho \int_x^0 dy \mathcal{I}_\varepsilon(x-y) \mathcal{A}(y), \quad (69)$$

where we used  $I_\varepsilon(x) = -I_\varepsilon(-x)$ . We get

$$\bar{\mathcal{A}}(x) = \frac{\pi_\rho}{2\bar{\nu}} \mathcal{A}(x) \left( \frac{e^{(\nu-\bar{\nu})x}}{\nu-\bar{\nu}} - \frac{e^{(\nu+\bar{\nu})x}}{\nu+\bar{\nu}} \right). \quad (70)$$

Finally, using the solution (46) of Eq. (44), where the function  $\hat{\Pi}_H^{\text{IR}}(s, p')$  always appears with the same second argument as  $\hat{I}_F^{\text{IR}}(p, p')$ , we conclude that the latter also factorizes:

$$\hat{I}_F^{\text{IR}}(p, p') = \frac{\pi_F}{\sqrt{pp'}} \bar{\mathcal{A}} \left( \ln \frac{p}{\mu} \right) \bar{\mathcal{A}} \left( \ln \frac{p'}{\mu} \right), \quad (71)$$

with the function  $\bar{\mathcal{A}}$  given in Eq. (70) above. The factorization property (71) of  $\hat{I}_F^{\text{IR}}$  follows directly from the factorization of  $\hat{\Pi}_F^{\text{IR}}$ , Eq. (66). As described in Appendix C, the latter follows from the corresponding factorization property (47) of the statistical correlator  $F_{\text{IR}}$  and is thus reminiscent of the fact that IR de Sitter fluctuations can be described as a classical stochastic ensemble of growing modes<sup>4</sup> [57–59].

Let us discuss in more detail the above solution, Eq. (71). Recalling that  $\bar{\nu} < \nu$ , one finds, for  $-x \gg 1$ ,

$$\bar{\mathcal{A}}(x) \approx \frac{\pi_\rho \mu^{\bar{\nu}-\nu}}{2\bar{\nu}(\nu-\bar{\nu})} \frac{e^{-\bar{\kappa}x}}{\mu^{\bar{\kappa}}} \approx \frac{e^{-\bar{\kappa}x}}{\mu^{\bar{\kappa}}}, \quad (72)$$

where we neglected terms of relative order  $\mathcal{O}(\pi_\rho)$  in the second equality. Here, we introduced the new exponent

$$\bar{\kappa} = \bar{\nu} - \varepsilon. \quad (73)$$

Again, we find that the infinite summation of bubble diagrams changes the IR power law of the single bubble

$$\mathcal{A} \left( \ln \frac{p}{\mu} \right) = \frac{1}{p^\kappa} \quad \longrightarrow \quad \bar{\mathcal{A}} \left( \ln \frac{p}{\mu} \right) \approx \frac{1}{p^{\bar{\kappa}}} \quad (74)$$

and  $\bar{\kappa} - \kappa$  can be regarded as an anomalous dimension. We thus have

$$\hat{I}_F^{\text{IR}}(p, p') \approx \frac{\pi_F}{(pp')^{\bar{\kappa} + \frac{1}{2}}}. \quad (75)$$

We emphasize that the dependence of the above results on the scale  $\mu \lesssim 1$  is quite mild  $\propto \mu^{\bar{\nu}-\nu} \approx 1 - \frac{\pi_\rho}{2\nu} \ln \mu$ , in the case  $\pi_\rho \ll 1$ . This suggests that the neglect of high momentum modes in the present analysis is a consistent approximation.

As in the case of  $\hat{I}_\rho$ , it is instructive to compare the exact solution (72) to the perturbative expansion in powers of  $\pi_\rho$ . Using (60), Eq. (69) reads, at lowest nontrivial order,

$$\begin{aligned} \bar{\mathcal{A}}(x) &= \mathcal{A}(x) + \pi_\rho \int_x^0 dy \mathcal{P}_\varepsilon(x-y) \mathcal{A}(y) + \mathcal{O}(\pi_\rho^2) \\ &= \mathcal{A}(x) \left( 1 + \frac{\pi_\rho}{2\nu} \left[ x + \frac{1}{2\nu} - \frac{e^{2\nu x}}{2\nu} \right] + \mathcal{O}(\pi_\rho^2) \right). \end{aligned} \quad (76)$$

<sup>4</sup> The fact that the connected two-point function factorizes is also to be put in parallel with the phenomenon of undulation in (analog) black hole physics [60]. In the present case, the undulation occurs in physical momentum space.

For IR momenta,  $-x = \ln(\mu/p) \gg 1$ , we get

$$\bar{\mathcal{A}}(x) \approx \mathcal{A}(x) \left( 1 + \frac{\pi_\rho}{2\nu} x + \mathcal{O}(\pi_\rho^2) \right). \quad (77)$$

We see that the true expansion parameter is, in fact,  $\pi_\rho \ln \mu/p$  and that, for momenta  $\ln(\mu/p) \gtrsim 1/\pi_\rho$ , one needs to resum the IR logarithms generated by the series of bubble diagrams. This results in the modification of the IR exponent  $\kappa \rightarrow \bar{\kappa}$ .

## VI. DISCUSSION

In the previous sections, we have mainly considered the case of a small, or vanishing, tree-level square mass  $m_{\text{dS}}^2 \rightarrow 0$ . In this case, perturbation theory suffers from strong IR divergences. As previously emphasized, one has, in that case,  $\varepsilon \propto \sqrt{\lambda}$  and thus  $\pi_\rho \propto \sqrt{\lambda}$ . The actual expansion parameter is thus  $\sqrt{\lambda}$ . The mass generation phenomenon discussed in Sec. IV can be viewed as a sort of anomalous dimension in the IR [36]. Indeed the IR power law behavior of the free propagator of a massless field, characterized by the exponent  $d/2$ , is changed to an exponent  $\nu \approx d/2 - \varepsilon$  which regulates the IR divergences of the perturbative series.

Similarly, the resummation of nonlocal IR logarithms in the two-point function of the composite operator  $\varphi^2$  or, equivalently, in the four-point vertex function of the field  $\varphi$  leads to a modified IR behavior: the power law behaviors of the one-loop bubble contributions  $\hat{\Pi}_\rho$  and  $\hat{\Pi}_F$ , characterized by the exponents  $\nu \approx d/2 - \varepsilon$  and  $\kappa \approx d/2 - 2\varepsilon$ , are changed to  $\bar{\nu} \approx d/2 - 3\varepsilon$  and  $\bar{\kappa} \approx d/2 - 4\varepsilon$  respectively.

We point out that, inversely, the dynamically generated IR power law behavior of the function  $\hat{D}$ , for large (super-Hubble) momentum/time separations  $|\ln p/p'| = |t-t'| \gtrsim 1$ , can be viewed as the generation of an effective mass for the composite field  $\varphi^2$ . Using, see (73),

$$e^{-\varepsilon|x|} \sinh \bar{\nu} x \approx \sinh \bar{\kappa} x, \quad \text{for } |x| \gtrsim 1, \quad (78)$$

as well as the relation (57) between  $\pi_F$  and  $\pi_\rho$ , one has, for  $|\ln p/p'| \gtrsim 1$ ,

$$pp' \hat{D}_F^{\text{IR}}(p, p') \approx \frac{\lambda \pi_\rho}{3N} \sqrt{pp'} \frac{F_{\bar{\kappa}}}{(pp')^{\bar{\kappa}}} \quad (79)$$

$$pp' \hat{D}_\rho^{\text{IR}}(p, p') \approx -\frac{\lambda \pi_\rho}{3N} \sqrt{pp'} \mathcal{P}_{\bar{\kappa}} \left( \ln \frac{p}{p'} \right). \quad (80)$$

We have assumed  $\varepsilon \ll 1$  and  $\pi_\rho \ll 1$ . In this case, one can identify  $\bar{\kappa} \approx \bar{\nu} \approx \nu$  in the constant factors on the right-hand side. Using Eq. (49), we see that the function  $pp' \hat{D}^{\text{IR}}(p, p')$  behaves as the two-point function of a free massive field with square mass  $\bar{M}^2 = d^2/4 - \bar{\kappa}^2$ . For vanishing tree-level mass, we get  $\bar{M} \approx 2M$ .

There is another interesting situation to be mentioned, namely the case of a negative tree-level square mass  $m_{\text{dS}}^2 < 0$ . This is the case where the classical potential

shows spontaneous symmetry breaking. In that case, perturbation theory is again ill-defined because of the presence of massless Goldstone modes. It has been shown in [33] that, as in the previous case, nonperturbative effects of self-interactions cure the theory by generating a positive mass square restoring the symmetry. The self-consistent mass is approximately given by

$$M^2 = \frac{m_{\text{dS}}^2}{2} + \sqrt{\frac{(m_{\text{dS}}^2)^2}{4} + \frac{\lambda F_\nu}{12} \frac{d\Omega_d}{(2\pi)^d}} \approx \frac{\lambda F_\nu}{12|m_{\text{dS}}^2|} \frac{d\Omega_d}{(2\pi)^d}, \quad (81)$$

from which it follows that

$$\varepsilon = \frac{\lambda F_\nu}{12|m_{\text{dS}}^2|} \frac{d\Omega_d}{(2\pi)^d} \quad (82)$$

and thus

$$\pi_\rho = 2|m_{\text{dS}}^2|. \quad (83)$$

This is equal to the radial curvature of the tree-level potential at its minimum. We see that, in that case,  $\varepsilon \propto \lambda$  is parametrically smaller than in the case of vanishing tree-level mass, leading to stronger IR enhancement and to a truly nonperturbative value of the parameter  $\pi_\rho$  governing the bubble resummation. At weak coupling, we get  $\bar{M} \approx \sqrt{\pi_\rho} \gg M$ . The composite field  $\varphi^2$  gets a nonperturbatively large mass.

## VII. CONCLUSIONS

Resumming perturbative IR divergences of QFT on de Sitter space is a timely issue of modern cosmology. The present study provides an exact solution of a nonperturbative limit where large IR logarithms can be explicitly resummed. This gives rise to modified power laws for the correlators in the IR, akin to anomalous dimensions in the context of critical phenomena.

A detailed analysis of the role of UV modes reveals that they only affect the IR results by a multiplicative constant. This is a form of effective decoupling between UV and IR physics in de Sitter space. That such a decoupling occurs in an expanding background is a highly nontrivial result.

The results obtained here in the large- $N$  limit are new exact results in the context of QFT on de Sitter. Since the early work of Starobinsky and Yokoyama [12], nonperturbative calculations have been rather scarce, owing to the difficulty of extending to de Sitter space standard flat space-time resummation or nonperturbative techniques. The situation has improved in recent years with, in particular, the use of the dynamical renormalization group approach [15], explicit QFT calculations in various nonperturbative approximation schemes [31, 33–36], all orders perturbative results [21, 22, 61], and resummation of Schwinger-Dyson equations [32, 40, 41, 62]. Also worth mentioning is the interesting proposal for a reorganized perturbative expansion in the context of Euclidean de Sitter space proposed in [37, 38].



We believe the methods proposed here and in [39] provide a powerful tool to pursue these studies. In particular, they are well suited to the study of the IR properties of de Sitter correlators and are in principle applicable to other approximation schemes. Examples presently under study include  $1/N$  corrections to the two-point function in the  $O(N)$  model and approximations based on two-particle-irreducible techniques [63].

### Acknowledgements

We acknowledge useful discussions with X. Busch, M. Garny, F. Gautier and U. Reinosa.

### Appendix A: Proof of Eq. (46)

Consider the integral on the right-hand side of Eq. (46) and use Eq. (44) to eliminate  $\hat{\Pi}_H$ :

$$\int_p^\infty ds \hat{I}_\rho(p, s) \hat{\Pi}_H(s, p') = \int_p^\infty ds \hat{I}_\rho(p, s) \hat{I}_F(s, p') - \int_p^\infty ds \int_s^\infty ds' \hat{I}_\rho(p, s) \hat{\Pi}_\rho(s, s') \hat{I}_F(s', p'). \quad (\text{A1})$$

Writing the double integral on the right-hand side as

$$\int_p^\infty ds \int_s^\infty ds' = \int_p^\infty ds' \int_p^{s'} ds \quad (\text{A2})$$

and using Eq. (43), the second line of Eq. (A1) rewrites as

$$- \int_p^\infty ds' \int_p^{s'} ds \hat{I}_\rho(p, s) \hat{\Pi}_\rho(s, s') \hat{I}_F(s', p') = \int_p^\infty ds' \left\{ \hat{\Pi}_\rho(p, s') - \hat{I}_\rho(p, s') \right\} \hat{I}_F(s', p'). \quad (\text{A3})$$

We thus get

$$\int_p^\infty ds \hat{I}_\rho(p, s) \hat{\Pi}_H(s, p') = \int_p^\infty ds \hat{\Pi}_\rho(p, s) \hat{I}_F(s, p'), \quad (\text{A4})$$

hence Eq. (46).

### Appendix B: Two-point correlators

In this series of appendices, we discuss various technical aspects of the present work. Appendices B and C present material directly used in the main body of the paper, in particular the calculation of the one-loop bubble functions  $\hat{\Pi}_F^{\text{IR}}$  and  $\hat{\Pi}_\rho^{\text{IR}}$ , Eqs. (54)-(55). The remaining Appendices D–G provide a detailed discussion of the role of high momenta (Appendix F), including the question of renormalization (Appendix G), in the case  $D = d+1 = 4$ ,

where the theory (7) is perturbatively renormalizable. This requires the evaluation of the functions  $\hat{\Pi}_{F,\rho}^{\text{mix}}$  and  $\hat{\Pi}_{F,\rho}^{\text{UV}}$ , defined below and discussed in Appendices D and E respectively.

In the present section, we recall the form of the statistical and spectral two-point functions and their approximate forms in the IR and UV limits. As in the main text, we separate the two regimes with an arbitrary scale  $\mu \sim 1$ . For a generic two-point function  $\mathcal{D}(p, p')$ , we introduce the notations

$$\mathcal{D}^{\text{IR}}(p, p') = \mathcal{D}(p \lesssim \mu, p' \lesssim \mu), \quad (\text{B1})$$

$$\mathcal{D}^{\text{UV}}(p, p') = \mathcal{D}(p \gtrsim \mu, p' \gtrsim \mu), \quad (\text{B2})$$

for the cases where both momenta are IR or UV and

$$\mathcal{D}^{\text{mix}}(p, p') = \mathcal{D}(p \lesssim \mu, p' \gtrsim \mu), \quad (\text{B3})$$

$$\mathcal{D}^{\text{xim}}(p, p') = \mathcal{D}(p \gtrsim \mu, p' \lesssim \mu), \quad (\text{B4})$$

for the cases where one momentum is IR and the other is UV. Notice that for (anti)symmetric functions  $\mathcal{D}(p, p') = \pm \mathcal{D}(p', p)$ , one has  $\mathcal{D}^{\text{mix}}(p, p') = \pm \mathcal{D}^{\text{xim}}(p', p)$ .

The statistical and spectral two-point functions of a free scalar field of mass  $M$  in the Bunch-Davies vacuum are given by

$$\hat{F}(p, p') = \frac{\pi}{4} \sqrt{pp'} \operatorname{Re} \{ H_\nu(p) H_\nu^*(p') \}, \\ \hat{\rho}(p, p') = -\frac{\pi}{2} \sqrt{pp'} \operatorname{Im} \{ H_\nu(p) H_\nu^*(p') \}, \quad (\text{B5})$$

with  $\nu = \sqrt{d^2/4 - M^2}$ . In the next sections we shall use the propagator (6) with both  $p$  and  $p'$  on the upper branch  $\hat{\mathcal{C}}^+$  of the contour  $\hat{\mathcal{C}}$ , where  $\operatorname{sign}_{\hat{\mathcal{C}}}(p - p') = -\operatorname{sign}(p - p')$  and thus

$$\hat{G}(p, p') = \hat{F}(p, p') + \frac{i}{2} \operatorname{sign}(p - p') \hat{\rho}(p, p') \quad \text{for } p, p' \in \hat{\mathcal{C}}^+. \quad (\text{B6})$$

We recall the symmetry relations  $\hat{G}(p, p') = \hat{G}(p', p)$ ,  $\hat{F}(p, p') = \hat{F}(p', p)$  and  $\hat{\rho}(p, p') = -\hat{\rho}(p', p)$ .

We are concerned here with the small mass case  $M \lesssim 1$  for which the index  $\nu$  is real. The leading low and high momentum behaviors of the Hankel function are given by [56]

$$H_\nu(p) \sim \frac{\Gamma(\nu)}{i\pi} \left( \frac{2}{p} \right)^\nu \equiv -i \sqrt{\frac{4}{\pi p}} f_\nu(p), \quad \text{for } p \ll 1, \quad (\text{B7})$$

where the second relation defines the function  $f_\nu(p)$ , and

$$H_\nu(p) \sim \sqrt{\frac{2}{\pi p}} e^{i(p - \varphi_\nu)}, \quad \text{for } p \gg 1, \quad (\text{B8})$$

where  $\varphi_\nu = \frac{\pi}{2}(\nu + \frac{1}{2})$ .

The IR behavior of the statistical function is readily obtained as

$$\hat{F}_{\text{IR}}(p, p') = f_\nu(p) f_\nu(p') = \frac{F_\nu}{(pp')^{\nu - \frac{1}{2}}}, \quad (\text{B9})$$

where  $F_\nu = [2^\nu \Gamma(\nu)]^2 / 4\pi$ . The factorization property (B9) expresses the (approximate [64]) classical nature and the phase coherence of IR fluctuations in de Sitter [57, 59]. The leading IR behavior of the spectral function necessitates a more precise calculation. It can be written as

$$\begin{aligned}\hat{\rho}_{\text{IR}}(p, p') &= -\frac{\sqrt{pp'}}{2\nu} \left[ \left(\frac{p}{p'}\right)^\nu - \left(\frac{p'}{p}\right)^\nu \right] \\ &= -\sqrt{pp'} \mathcal{P}_\nu \left( \ln \frac{p}{p'} \right),\end{aligned}\quad (\text{B10})$$

where we introduced the function  $\mathcal{P}_\nu$  of (50). The mixed components are obtained from (B7), (B8)

$$\hat{F}_{\text{mix}}(p, p') = -f_\nu(p) \frac{\sin(p' - \varphi_\nu)}{\sqrt{2}}, \quad (\text{B11})$$

$$\hat{\rho}_{\text{mix}}(p, p') = 2f_\nu(p) \frac{\cos(p' - \varphi_\nu)}{\sqrt{2}}, \quad (\text{B12})$$

or, equivalently,

$$\hat{G}_{\text{mix}}(p, p') = f_\nu(p) \frac{e^{-i(p' - \varphi_\nu)}}{i\sqrt{2}}, \quad \text{for } p, p' \in \hat{\mathcal{C}}^+. \quad (\text{B13})$$

Finally, the UV components have the following Minkowski-like expressions (with physical momentum in place of time)

$$\hat{F}_{\text{UV}}(p, p') = \frac{1}{2} \cos(p - p'), \quad (\text{B14})$$

$$\hat{\rho}_{\text{UV}}(p, p') = -\sin(p - p'), \quad (\text{B15})$$

or, equivalently,

$$\hat{G}_{\text{UV}}(p, p') = \frac{e^{-i|p-p'|}}{2}, \quad \text{for } p, p' \in \hat{\mathcal{C}}^+. \quad (\text{B16})$$

In the deep UV regime  $p, p' \gg 1$  and for subhorizon time separation  $|\ln p/p'| = |t - t'| \ll 1$ , one has  $p - p' \approx -p(t - t')$  (recall that  $p'e^{t'} = pe^t$ ) and one recovers the (massless) Minkowski vacuum correlator

$$\frac{\hat{G}_{\text{UV}}(p, p')}{\sqrt{pp'}} \approx \frac{e^{-ip|t-t'|}}{2p}. \quad (\text{B17})$$

### Appendix C: Calculation of $\hat{\Pi}^{\text{IR}}(p, p')$

Here, we compute the leading IR behavior of the one-loop bubble function  $\hat{\Pi}(p, p')$ , defined in (38). It is sufficient to consider the case where both  $p$  and  $p'$  lie on the upper branch  $\hat{\mathcal{C}}^+$  of the contour and  $p < p'$ , such that  $\text{sign}_{\hat{\mathcal{C}}}(p - p') = 1$ . We separate the momentum integral in three regions: low momentum modes, such that  $qp < qp' \lesssim \mu$ ; intermediate momentum modes with  $qp \lesssim \mu \lesssim qp'$ ; and high momentum modes with  $\mu \lesssim qp < qp'$ .

### 1. IR contribution

The contribution from low momentum, IR modes gives the dominant contribution. One needs to consider the  $F$  and  $\rho$  components, Eqs. (41) and (42) separately. Here, the condition  $qp < qp' \lesssim \mu$  implies that  $rp < rp' \lesssim \mu$  and both propagators under the loop integral can be approximated by their IR behavior, Eqs. (B9) and (B10). In that case, due to the strong IR enhancement of the statistical propagator as compared to the spectral one, one can safely neglect the (quantum) contribution  $\hat{\rho}\hat{\rho}$  as compared to the (classical) one<sup>5</sup>  $\hat{F}\hat{F}$  in  $\hat{\Pi}_F$ . We get

$$\begin{aligned}\hat{\Pi}_F^{\text{IR}}(p, p') &\approx -\frac{\lambda}{6} (pp')^{\frac{d-3}{2}} \int_{|\mathbf{q}| < \frac{\mu}{p'}} \frac{\hat{F}_{\text{IR}}(qp, qp') \hat{F}_{\text{IR}}(rp, rp')}{qr} \\ &\approx -\frac{\lambda}{6} (pp')^{\frac{d-3}{2}} \hat{F}_{\text{IR}}^2(p, p') \int_{\mathbf{q}} \frac{1}{(qr)^{2\nu}},\end{aligned}\quad (\text{C1})$$

for the  $F$  component and

$$\begin{aligned}\hat{\Pi}_\rho^{\text{IR}}(p, p') &\approx -\frac{\lambda}{3} (pp')^{\frac{d-3}{2}} \int_{|\mathbf{q}| < \frac{\mu}{p'}} \frac{\hat{F}_{\text{IR}}(qp, qp') \hat{\rho}_{\text{IR}}(rp, rp')}{qr} \\ &= -\frac{\lambda}{3} (pp')^{\frac{d-3}{2}} \hat{F}_{\text{IR}}(p, p') \hat{\rho}_{\text{IR}}(p, p') \int_{|\mathbf{q}| < \frac{\mu}{p'}} \frac{1}{q^{2\nu}},\end{aligned}\quad (\text{C2})$$

for the  $\rho$  component, where we recall that  $r = |\mathbf{e} + \mathbf{q}|$  with  $\mathbf{e}$  an arbitrary unit vector. Since the momentum integral in the second line of Eq. (C1) converges rapidly at large momentum ( $2\nu \approx d$ ) we can safely ignore the upper bound. One cannot do so in the momentum integral in the second line of Eq. (C2) since the latter is sensitive to the upper bound. This results in a nontrivial  $p'/p$  dependence, as discussed below.

The integral in Eq. (C1) is easily evaluated by using the technique of Feynman parameters. We write

$$\frac{1}{(qr)^{2\nu}} = \frac{\Gamma(2\nu)}{\Gamma^2(\nu)} \int_0^1 dx \frac{[x(1-x)]^{\nu-1}}{[xq^2 + (1-x)r^2]^{2\nu}} \quad (\text{C3})$$

and  $xq^2 + (1-x)r^2 = [\mathbf{q} + (1-x)\mathbf{e}]^2 + x(1-x)$ . Performing the shift  $\mathbf{q} + (1-x)\mathbf{e} \rightarrow \mathbf{q}$  under the  $\mathbf{q}$  integration, one can perform all the angular integrations in  $d$ -dimensional spherical coordinates, to get

$$\int_{\mathbf{q}} \frac{1}{(qr)^{2\nu}} = \frac{\Omega_d}{(2\pi)^d} \frac{\Gamma(2\nu)}{\Gamma^2(\nu)} \int_0^1 dx \int_0^\infty dq \frac{q^{d-1} [x(1-x)]^{\nu-1}}{[q^2 + x(1-x)]^{2\nu}}, \quad (\text{C4})$$

where  $\Omega_d = 2\pi^{d/2}/\Gamma(d/2)$ . Finally, performing the change of variable  $u = q^2/x(1-x)$ , the  $u$  and  $x$  integration can be trivially performed. We obtain, recalling

<sup>5</sup> This is a typical classical (statistical) field approximation [7, 65, 66].

$$\nu = d/2 - \varepsilon,$$

$$\begin{aligned} \int_{\mathbf{q}} \frac{1}{(qr)^{2\nu}} &= \frac{\Omega_d}{(2\pi)^d} \frac{\Gamma(\frac{d}{2}) \Gamma(\frac{d}{2} - 2\varepsilon)}{\Gamma^2(\frac{d}{2} - \varepsilon)} \frac{\Gamma^2(\varepsilon)}{2\Gamma(2\varepsilon)} \\ &= \frac{\Omega_d}{(2\pi)^d} \frac{1}{\varepsilon} \left[1 + \mathcal{O}(\varepsilon)\right]. \end{aligned} \quad (\text{C5})$$

The leading IR behavior is then

$$\hat{\Pi}_F^{\text{IR}}(p, p') = \frac{\pi_F}{(pp')^{\kappa + \frac{1}{2}}} \quad (\text{C6})$$

with  $\kappa = \frac{d}{2} - 2\varepsilon = \nu - \varepsilon < \nu$  and

$$\pi_F = -\frac{\lambda F_\nu^2}{6\varepsilon} \frac{\Omega_d}{(2\pi)^d}. \quad (\text{C7})$$

As already emphasized below Eq. (66), the function  $\hat{\Pi}_F^{\text{IR}}$  assumes a factorized form which is reminiscent of the classical coherent nature of IR de Sitter fluctuations. For later use we rewrite  $\hat{\Pi}_F^{\text{IR}}$  as

$$\hat{\Pi}_F^{\text{IR}}(p, p') = A(p)A(p'), \quad (\text{C8})$$

where the function  $A$  is related to the one introduced in (67) as

$$A(p) = \frac{i\sqrt{-\pi_F}}{p^{\kappa + \frac{1}{2}}} = i\sqrt{\frac{-\pi_F}{p}} \mathcal{A}\left(\ln \frac{p}{\mu}\right). \quad (\text{C9})$$

The integral in Eq. (C2) is easily performed:

$$\begin{aligned} \int_{|\mathbf{q}| < \frac{\mu}{p'}} \frac{1}{q^{2\nu}} &= \frac{\Omega_d}{(2\pi)^d} \frac{1}{2\varepsilon} \left(\frac{\mu}{p'}\right)^{2\varepsilon} \\ &= \frac{\Omega_d}{(2\pi)^d} \frac{(p')^{-2\varepsilon}}{2\varepsilon} \left[1 + \mathcal{O}(\varepsilon)\right], \end{aligned} \quad (\text{C10})$$

which leads to

$$\hat{\Pi}_\rho^{\text{IR}}(p, p') = \frac{\pi_\rho}{\sqrt{pp'}} \left(\frac{p}{p'}\right)^\varepsilon \mathcal{P}\left(\ln \frac{p}{p'}\right) \quad \text{for } p < p', \quad (\text{C11})$$

where

$$\pi_\rho = \frac{\lambda F_\nu}{6\varepsilon} \frac{\Omega_d}{(2\pi)^d}. \quad (\text{C12})$$

Using the antisymmetry of the function  $\hat{\Pi}_\rho(p, p')$ , we have then

$$\hat{\Pi}_\rho^{\text{IR}}(p, p') = \frac{\pi_\rho}{\sqrt{pp'}} \left(\frac{p'}{p}\right)^\varepsilon \mathcal{P}\left(\ln \frac{p}{p'}\right) \quad \text{for } p > p'. \quad (\text{C13})$$

From this we get Eq. (55).

## 2. Mixed and UV contributions

We now show that the intermediate and high momentum contributions to  $\hat{\Pi}^{\text{IR}}$  are subleading in the limit  $p, p' \ll 1$ . The contribution from intermediate momenta  $qp \lesssim \mu \lesssim qp'$  is such that  $q \gtrsim \mu/p' \gg 1$ , which implies that  $r \approx q \gg 1$  and thus  $rp \lesssim 1 \lesssim rp'$ . It follows that both propagators in Eq. (38) can be replaced by their ‘‘mixed’’ expression (B13). We thus have to evaluate the integral

$$\begin{aligned} &\int_{\frac{\mu}{p'} < |\mathbf{q}| < \frac{\mu}{p}} \frac{G_{\text{mix}}(qp, qp') \hat{G}_{\text{mix}}(rp, rp')}{qr} \\ &= \frac{F_{\text{IR}}(p, p')}{2} \int_{\frac{\mu}{p'} < |\mathbf{q}| < \frac{\mu}{p}} \frac{e^{-i[(q+r)p' - 2\varphi_\nu]}}{(qr)^{\nu + \frac{1}{2}}} \\ &\approx \frac{\Omega_d}{(2\pi)^d} \frac{F_{\text{IR}}(p, p')}{2} \int_{\frac{\mu}{p'}}^{\frac{\mu}{p}} \frac{dq}{q^2} e^{-2i(qp' - \varphi_{d/2})}, \end{aligned} \quad (\text{C14})$$

where we can safely replace  $\nu \rightarrow d/2$  in the last line. The remaining integral is bounded:

$$\left| \int_{\frac{\mu}{p'}}^{\frac{\mu}{p}} \frac{dq}{q^2} e^{-2i(qp' - \varphi_\nu)} \right| < \int_{\frac{\mu}{p'}}^{\frac{\mu}{p}} \frac{dq}{q^2} = \frac{p' - p}{\mu} \quad (\text{C15})$$

and one easily checks that the corresponding contributions to either  $\hat{\Pi}_F^{\text{IR}} = \text{Re} \hat{\Pi}^{\text{IR}}$  or  $\hat{\Pi}_\rho^{\text{IR}} = -2i \text{Im} \hat{\Pi}^{\text{IR}}$  are negligible as compared to those obtained in the previous subsection (notice also that there is no IR enhancement factor  $1/\varepsilon$ ).

Finally, the high momentum contribution can be estimated along similar lines. In  $D \geq 4$  the integral diverges for  $p' \rightarrow p$  and needs to be regulated. Here, we regulate the theory by imposing a sharp cutoff  $\Lambda$  on physical momenta, i.e. by effectively replacing the propagators  $G(p, p') \rightarrow G(p, p')\theta(\Lambda - p)\theta(\Lambda - p')$ , see Appendix G. We thus have  $\mu \lesssim qp < qp' < \Lambda$  and, therefore,  $q \gg 1$ , so that  $r \approx q \gg 1$  and  $rp' > rp \gtrsim \mu$ . Both propagators in (38) can thus be replaced by their UV expression (B16). The corresponding contribution reads

$$\begin{aligned} &\int_{\frac{\mu}{p} < |\mathbf{q}| < \frac{\Lambda}{p}} \frac{\hat{G}_{\text{UV}}(qp, qp') \hat{G}_{\text{UV}}(rp, rp')}{qr} \\ &= \frac{1}{4} \int_{\frac{\mu}{p} < |\mathbf{q}| < \frac{\Lambda}{p}} \frac{e^{i(q+r)[p-p']}}{qr} \\ &\approx \frac{\Omega_d}{4(2\pi)^d} \int_{\frac{\mu}{p}}^{\frac{\Lambda}{p}} \frac{dq}{q^{3-d}} e^{2iq(p-p')}. \end{aligned} \quad (\text{C16})$$

Again an upper bound is given by

$$\left| \int_{\frac{\mu}{p}}^{\frac{\Lambda}{p}} \frac{dq}{q^{3-d}} e^{2iq(p-p')} \right| < \int_{\frac{\mu}{p}}^{\frac{\Lambda}{p}} \frac{dq}{q^{3-d}} = \frac{\left(\frac{\Lambda}{p}\right)^{d-2} - \left(\frac{\mu}{p}\right)^{d-2}}{d-2}, \quad (\text{C17})$$

which is easily shown to give negligible contributions to both  $\hat{\Pi}_F^{\text{IR}}$  and  $\hat{\Pi}_\rho^{\text{IR}}$  in the low momentum limit  $p, p' \ll 1$ , at fixed cutoff  $\Lambda$ .

We end this subsection with a more precise evaluation of the UV contribution (C16), useful for our discussion of renormalization in Appendix G. One has, for  $p \ll 1$  and  $x = p - p'$  finite,

$$\int_{\frac{\mu}{p}}^{\frac{\Lambda}{p}} \frac{dq}{q^{3-d}} e^{2iqx} \approx \left(\frac{p}{\Lambda}\right)^{3-d} \frac{e^{2i\frac{\Lambda}{p}x}}{2ix} - \left(\frac{p}{\mu}\right)^{3-d} \frac{e^{2i\frac{\mu}{p}x}}{2ix}. \quad (\text{C18})$$

We see that, as expected, that the one-loop bubble—which we recall is a one-loop contribution to the four-point vertex function—is finite in the limit  $\Lambda \rightarrow \infty$  for  $D = d + 1 \leq 3$ , where the present theory is super-renormalizable, and has no coupling divergence. The case  $D = 4$ , where the theory is (perturbatively) renormalizable, requires a more careful analysis, which is performed in Sec. G. For a larger number of dimensions, the one-loop bubble exhibits a strong cutoff dependence.

#### Appendix D: Calculation of $\hat{\Pi}^{\text{mix}}(p, p')$

For our discussion of the role of high momentum (sub-horizon) modes to the integral equations (43)-(45) in Appendix F below, we shall need both the mixed ( $p \lesssim \mu \lesssim p'$ ) and UV ( $\mu \lesssim p, p'$ ) behaviors of the one-loop bubble  $\hat{\Pi}(p, p')$  for large  $p'$ . We analyze the former in detail here, specializing to  $d = 3$  spatial dimensions.

By definition, see Eq. (B3), the mixed contribution  $\hat{\Pi}^{\text{mix}}(p, p')$  is such that  $p < p'$ . The propagator (B6) thus reads

$$\hat{G}(p, p') = \frac{\pi}{4} \sqrt{pp'} H_\nu(p) H_\nu^*(p'). \quad (\text{D1})$$

By choosing  $q = |\mathbf{q}|$  and  $r = |\mathbf{e} + \mathbf{q}|$  as integration variables, the loop integral (38) can be written as

$$\hat{\Pi}(p, p') = -\frac{\lambda}{24\pi^2} J(p, p'), \quad (\text{D2})$$

with

$$\begin{aligned} J(p, p') &= \int_0^\infty dq \hat{G}(qp, qp') \int_{|1-q|}^{1+q} dr \hat{G}(rp, rp') \\ &= \int_0^\infty dq \mathcal{H}(q, p, p') \left\{ \mathcal{F}(1+q, p, p') - \mathcal{F}(|1-q|, p, p') \right\}. \end{aligned} \quad (\text{D3})$$

In the second line we introduced the (redundant) notation

$$\mathcal{H}(q, p, p') = \hat{G}(qp, qp') \quad (\text{D4})$$

for later use. We exploit the fact that, in  $d = 3$ , the  $r$  integration can be performed explicitly using the indefinite

integral [36, 56]

$$\begin{aligned} \mathcal{F}(q, p, p') &= \int dq \hat{G}(qp, qp') = \\ &= \frac{\pi}{4} \sqrt{pp'} \frac{qp' H_\nu(qp) H_{\nu-1}^*(qp') - qp H_\nu^*(qp') H_{\nu-1}(qp)}{p^2 - p'^2} \\ &= -\hat{G}(qp, qp') \frac{\mathcal{R}_\nu(qp) - \mathcal{R}_\nu^*(qp')}{q(p^2 - p'^2)}, \end{aligned} \quad (\text{D5})$$

where we defined the function

$$\mathcal{R}_\nu(p) = \frac{p H_{\nu-1}(p)}{H_\nu(p)}. \quad (\text{D6})$$

The third line of Eq. (D5) is particularly useful when it comes to approximating the function  $\mathcal{F}(q, p, p')$  for low or large momenta. Indeed, the function  $\mathcal{R}_\nu(p)$  has the following simple limits:

$$\mathcal{R}_\nu(p \gg 1) \approx ip \quad \text{and} \quad \mathcal{R}_\nu(p \ll 1) \approx \frac{p^2}{2(\nu-1)}. \quad (\text{D7})$$

We are interested in the behavior of the function  $J(p, p')$  for  $p \ll 1 \ll p'$ . In the vanishing mass limit,  $\nu \rightarrow 3/2$ , the integral features IR divergences for  $qp' \lesssim 1$  and  $|1-q|p' \lesssim 1$  as can be seen from the low momentum behavior of the integrand, see e.g., Eqs. (D23) and (D24) below. Using a similar technique as in [7, 36], we separate the  $q$  integral in (D3) in four contributions<sup>6</sup>

$$\int_0^\infty = \int_0^{\frac{\mu}{p'}} + \int_{\frac{\mu}{p'}}^{1-\frac{\mu}{p'}} + \int_{1-\frac{\mu}{p'}}^{1+\frac{\mu}{p'}} + \int_{1+\frac{\mu}{p'}}^\infty, \quad (\text{D8})$$

with  $\mu \sim 1$ . Reorganizing the various terms and using some changes of variables, we arrive at

$$J(p, p') = \sum_{i=1}^4 J_i(p, p'), \quad (\text{D9})$$

where (omitting the implicit dependence on  $p$  and  $p'$  for brevity)

$$J_1 = \int_0^{\frac{\mu}{p'}} dq \mathcal{H}(q) \{ \mathcal{F}(1+q) - \mathcal{F}(1-q) \}, \quad (\text{D10})$$

$$J_2 = - \int_0^{\frac{\mu}{p'}} dq \mathcal{F}(q) \{ \mathcal{H}(1+q) + \mathcal{H}(1-q) \} \quad (\text{D11})$$

grab together all potentially IR dangerous contributions,

$$J_3 = \int_{\frac{\mu}{p'}}^\infty dq \{ \mathcal{H}(q) \mathcal{F}(1+q) - \mathcal{H}(1+q) \mathcal{F}(q) \} \quad (\text{D12})$$

—————

<sup>6</sup> Note that the integral is UV finite for  $p \neq p'$ , see Appendix G. We can safely send the upper bound to  $\infty$ .

and

$$J_4 = - \int_{\frac{\mu}{p'}}^{1-\frac{\mu}{p'}} dq \mathcal{H}(q) \mathcal{F}(1-q). \quad (\text{D13})$$

In the following, we adopt a similar notation as the one introduced in Appendix B for two-point functions to distinguish the various regimes in  $q$  of the functions  $\mathcal{H}$  and  $\mathcal{F}$ . For instance we note  $\mathcal{H}(q, p, p')$  as

$$\mathcal{H}_{\text{IR}}(q, p, p') \quad \text{for} \quad qp, qp' \lesssim \mu, \quad (\text{D14})$$

$$\mathcal{H}_{\text{mix}}(q, p, p') \quad \text{for} \quad qp \lesssim \mu \lesssim qp', \quad (\text{D15})$$

$$\mathcal{H}_{\text{UV}}(q, p, p') \quad \text{for} \quad \mu \lesssim qp, qp', \quad (\text{D16})$$

and similarly for  $\mathcal{F}(q, p, p')$ . With this notation, we have, for the IR contributions,

$$J_1 \approx \int_0^{\frac{\mu}{p'}} dq \mathcal{H}_{\text{IR}}(q) \{ \mathcal{F}_{\text{mix}}(1+q) - \mathcal{F}_{\text{mix}}(1-q) \} \quad (\text{D17})$$

and

$$J_2 \approx - \int_0^{\frac{\mu}{p'}} dq \mathcal{F}_{\text{IR}}(q) \{ \mathcal{H}_{\text{mix}}(1+q) + \mathcal{H}_{\text{mix}}(1-q) \}. \quad (\text{D18})$$

We separate the integral  $J_3$  in two contributions from intermediate  $qp \lesssim \mu \lesssim qp'$  and high  $\mu \lesssim qp, qp'$  momenta:

$$J_3 = J_3^{\text{mix}} + J_3^{\text{UV}}, \quad (\text{D19})$$

with

$$J_3^{\text{mix}} \approx \int_{\frac{\mu}{p'}}^{\frac{\mu}{p'}} dq \{ \mathcal{H}_{\text{mix}}(q) \mathcal{F}_{\text{mix}}(1+q) - \mathcal{H}_{\text{mix}}(1+q) \mathcal{F}_{\text{mix}}(q) \} \quad (\text{D20})$$

and

$$J_3^{\text{UV}} \approx \int_{\frac{\mu}{p}}^{\infty} dq \{ \mathcal{H}_{\text{UV}}(q) \mathcal{F}_{\text{UV}}(1+q) - \mathcal{H}_{\text{UV}}(1+q) \mathcal{F}_{\text{UV}}(q) \}. \quad (\text{D21})$$

Finally

$$J_4 \approx - \int_{\frac{\mu}{p'}}^{1-\frac{\mu}{p'}} dq \mathcal{H}_{\text{mix}}(q) \mathcal{F}_{\text{mix}}(1-q). \quad (\text{D22})$$

To evaluate the various integrals above, we use the leading IR and mix behaviors

$$\mathcal{H}_{\text{IR}}(q, p, p') \approx \frac{\hat{G}_{\text{IR}}(p, p')}{q^{2\nu-1}}, \quad (\text{D23})$$

$$\mathcal{F}_{\text{IR}}(q, p, p') \approx -q \mathcal{H}_{\text{IR}}(q, p, p') \quad (\text{D24})$$

and

$$\mathcal{H}_{\text{mix}}(q, p, p') \approx \sqrt{\frac{\hat{G}_{\text{IR}}(p, p')}{2}} \frac{e^{-i(qp' - \varphi_\nu)}}{iq^{\nu-\frac{1}{2}}}, \quad (\text{D25})$$

$$\mathcal{F}_{\text{mix}}(q, p, p') \approx \mathcal{H}_{\text{mix}}(q, p, p') \left( \frac{i}{p'} + q \frac{p^2}{p'^2} \right). \quad (\text{D26})$$

The UV contribution (D21) has no IR problem and can be safely evaluated by setting  $\nu \rightarrow 3/2$ . Using

$$H_{\frac{1}{2}}(p) = \sqrt{\frac{2}{\pi p}} \frac{e^{ip}}{i}, \quad H_{\frac{3}{2}}(p) = H_{\frac{1}{2}}(p) \left( \frac{1}{p} - i \right), \quad (\text{D27})$$

we get, after some calculations,

$$\mathcal{H}_{\text{UV}}(q) = \frac{e^{iq(p-p')}}{2} \left[ 1 + \frac{i}{q} \left( \frac{1}{p} - \frac{1}{p'} \right) + \frac{1}{qpp'} \right], \quad (\text{D28})$$

$$\mathcal{F}_{\text{UV}}(q) = \frac{e^{iq(p-p')}}{2i(p-p')} \left[ 1 + \frac{i}{q} \left( \frac{1}{p} - \frac{1}{p'} \right) \right]. \quad (\text{D29})$$

We thus have (recall that  $qp, qp' \gg 1$ )

$$\begin{aligned} & \mathcal{H}_{\text{UV}}(q) \mathcal{F}_{\text{UV}}(1+q) - \mathcal{H}_{\text{UV}}(1+q) \mathcal{F}_{\text{UV}}(q) \\ &= \frac{ie^{i(2q+1)(p-p')}}{4pp'(p'-p)} \frac{2q+1+i\left(\frac{1}{p}-\frac{1}{p'}\right)}{[q(q+1)]^2} \\ &\approx \frac{ie^{-i(2q+1)p'}}{4pp'^2} \frac{2}{q^3}. \end{aligned} \quad (\text{D30})$$

Notice that the high momentum  $q^{-3}$  behavior shows that, as expected, the integral  $J(p, p')$  is UV finite for  $p \neq p'$ .

Using the various approximations above in the relevant integrals and isolating the dominant contributions in the limit  $p \ll 1 \ll p'$ , we get, after some manipulations,

$$\begin{aligned} J_1 + J_2 &\approx i \hat{G}_{\text{IR}}(p, p) \frac{e^{-ip'}}{(p')^{1+\epsilon}} \int_0^\mu dx \frac{\sin x + x \cos x}{x^{1-2\epsilon}} \\ &\approx i \frac{\hat{G}_{\text{IR}}(p, p)}{\epsilon} \frac{e^{-ip'}}{(p')^{1+\epsilon}} \end{aligned} \quad (\text{D31})$$

and

$$\begin{aligned} J_4 &\approx i \hat{G}_{\text{IR}}(p, p) \frac{e^{-ip'}}{2p'} \int_{\frac{\mu}{p'}}^{1-\frac{\mu}{p'}} \frac{dq}{[q(1-q)]^{1-\epsilon}} \\ &\approx i \frac{\hat{G}_{\text{IR}}(p, p)}{\epsilon} \frac{e^{-ip'}}{p'} \left[ 1 - \left( \frac{1}{p'} \right)^\epsilon \right]. \end{aligned} \quad (\text{D32})$$

The contributions  $J_3^{\text{mix}}$  and  $J_3^{\text{UV}}$  are suppressed by relative factors  $\varepsilon p^2/p'$  and  $\varepsilon p^4/p'^2$  respectively. The IR contribution  $J_1 + J_2$  cancels the  $1/(p')^\epsilon$  contribution from  $J_4$  and we obtain, finally,

$$J(p, p') \approx i \frac{\hat{G}_{\text{IR}}(p, p)}{\epsilon} \frac{e^{-ip'}}{p'}. \quad (\text{D33})$$

We conclude that the mixed one-loop bubble  $\hat{\Pi}^{\text{mix}}$  assumes the factorized form

$$\hat{\Pi}^{\text{mix}}(p, p') \approx A(p) B(p'), \quad (\text{D34})$$

where the low momentum piece  $A(p)$  is the one characterizing the IR contribution (C8) with, here,  $\kappa+1/2 = 2-2\epsilon$  and  $\pi_F = -\lambda/48\pi^2\varepsilon$ , and the high momentum piece is given by

$$B(p) = -\sqrt{-\pi_F} \frac{e^{-ip}}{p}. \quad (\text{D35})$$

### Appendix E: Calculation of $\hat{\Pi}^{\text{UV}}(p, p')$

We shall also need the high momentum behavior of the one-loop bubble  $\hat{\Pi}^{\text{UV}}$ . We proceed along similar lines as in the previous section. As in the case of  $\hat{\Pi}^{\text{IR}}$  discussed in Appendix C, one needs to regulate the integral in the UV since it diverges for  $p' \rightarrow p$ . We employ the same regulator as before, namely a sharp cutoff on physical momenta. This essentially<sup>7</sup> amounts to cutting the  $q$  integration with a sharp cutoff  $\Lambda/\max(p, p')$ .

We shall see that  $\hat{\Pi}^{\text{UV}}(p, p')$  has a singular  $1/|p - p'|$  structure when  $p' \rightarrow p$ . For our present purposes, this function is essentially involved under integrals such as (39) which, we assume, are dominated by this singular structure. Therefore, we seek the leading singular contribution to  $\hat{\Pi}^{\text{UV}}(p, p')$ .

In the present case, where  $p, p' \gtrsim 1$ , potential IR contributions to the momentum integral in (D3) come from the regions (taking  $p < p'$ )  $q \lesssim \mu/p'$  and  $|1 - q| \lesssim \mu/p'$  as well as  $\mu/p' \lesssim q \lesssim \mu/p$  and  $\mu/p' \lesssim |1 - q| \lesssim \mu/p$ . However, these give regular contributions in the limit  $p' \rightarrow p$ . The remaining contributions can be separated in three pieces:

$$J_1^{\text{UV}} = - \int_{\frac{\mu}{p}}^{1 - \frac{\mu}{p}} dq \mathcal{H}_{\text{UV}}(q) \mathcal{F}_{\text{UV}}(1 - q), \quad (\text{E1})$$

$$J_2^{\text{UV}} = \int_{\frac{\mu}{p}}^{\frac{\Delta}{p}} dq \{ \mathcal{H}_{\text{UV}}(q) \mathcal{F}_{\text{UV}}(1 + q) - \mathcal{H}_{\text{UV}}(1 + q) \mathcal{F}_{\text{UV}}(q) \} \quad (\text{E2})$$

and

$$J_3^{\text{UV}} = \int_{\frac{\Delta}{p} - 1}^{\frac{\Delta}{p}} dq \mathcal{H}_{\text{UV}}(1 + q) \mathcal{F}_{\text{UV}}(q), \quad (\text{E3})$$

which can be safely evaluated by setting  $\nu \rightarrow 3/2$ , i.e., using Eqs. (D28)-(D30). We obtain, for the leading singular behavior when  $p' \rightarrow p$  (we also take  $\frac{\Delta}{p} \gg 1$ ),

$$J_1^{\text{UV}} \approx \frac{e^{i(p-p')}}{4i(p-p')}, \quad (\text{E4})$$

$$J_3^{\text{UV}} \approx \frac{e^{2i\frac{\Delta}{p}(p-p')}}{4i(p-p')} \frac{\sin(p-p')}{p-p'}, \quad (\text{E5})$$

whereas  $J_2^{\text{UV}} \approx J_1^{\text{UV}}/p$  receives a  $1/p$  suppression.

Considering also the case  $p > p'$ , our final result for the leading singular behavior of the function  $\hat{\Pi}^{\text{UV}}$  is

$$\hat{\Pi}^{\text{UV}}(p, p') = \frac{\lambda}{96i\pi^2} \left\{ \frac{e^{-i|x|}}{|x|} + \frac{e^{-2i\tilde{\Lambda}|x|} \sin x}{|x| x} \right\}, \quad (\text{E6})$$

<sup>7</sup> In principle, one should consider the fact that the cutoff also applies to  $r = |\mathbf{e} + \mathbf{q}|$ : there should be a term  $\theta(\Lambda - qp)\theta(\Lambda - qp')\theta(\Lambda - rp)\theta(\Lambda - rp')$  under the  $\mathbf{q}$  integral. However, the UV divergence arises from very high momenta where  $r \approx q$  and we neglect these subtleties here.

where  $x \equiv p - p'$  and  $\tilde{\Lambda} = \Lambda/\max(p, p')$ .

As in the case of the field correlator (B16), it is interesting to note that the UV behavior of the function  $\sqrt{pp'}\hat{\Pi}(p, p')$  assumes a Minkowski-like form with physical momenta in place of time. The Minkowski result  $\Pi_{\text{Mink}}(t-t', p)$  for the one-loop bubble—in the Minkowski vacuum—is recovered for  $p, p' \gg 1$  and  $|\ln p/p'| = |t - t'| \ll 1$ :

$$\hat{\Pi}_{\text{Mink}}(\Delta t, p) = \frac{\lambda}{96i\pi^2} \left\{ \frac{e^{-ip|\Delta t|}}{|\Delta t|} + \frac{e^{-2i\Lambda|\Delta t|} \sin p\Delta t}{|\Delta t| p\Delta t} \right\}, \quad (\text{E7})$$

where we used  $\tilde{\Lambda}|p - p'| \approx \Lambda|t - t'|$ .

### Appendix F: Influence of subhorizon modes

In this section, we present a complete solution of Eqs. (43)–(45) including high momentum modes. We show that the result (65) for the  $\rho$  component of the resummed function  $\hat{I}$  is not modified, whereas the  $F$  component (71) is only modified by a constant multiplicative factor of order unity.

The key observation for the present analysis is that the IR and mix behaviors of the one-loop bubble function  $\hat{\Pi}$ , Eqs. (C8) and (D34), have the factorized expressions

$$\hat{\Pi}_F^{\text{IR}}(p, p') = A(p)A(p') \quad (\text{F1})$$

and

$$\hat{\Pi}_F^{\text{mix}}(p, p') = A(p)B_F(p'), \quad \hat{\Pi}_\rho^{\text{mix}}(p, p') = A(p)B_\rho(p'), \quad (\text{F2})$$

where we recall the relation of the one-point function  $A(p)$  to the one used in the main text, see Eq. (67),

$$A(p) = i\sqrt{\frac{-\pi_F}{p}} \mathcal{A}\left(\ln \frac{p}{\mu}\right) \quad (\text{F3})$$

and where the functions  $B_{F,\rho}(p)$  are obtained from Eq. (D35):

$$B_F(p) = \text{Re } B(p) = -\sqrt{-\pi_F} \frac{\cos p}{p}, \quad (\text{F4})$$

$$B_\rho(p) = -2\text{Im } B(p) = -2\sqrt{-\pi_F} \frac{\sin p}{p}. \quad (\text{F5})$$

Let us first consider Eq. (44) for IR modes  $p, p' \ll 1$  and separate the  $s$  integral in a low momentum and a high momentum piece:  $\int_p^\infty = \int_p^\mu + \int_\mu^\infty$  with  $\mu \sim 1$ . Using the notation (B1)–(B4), we thus write

$$\begin{aligned} \hat{I}_F^{\text{IR}}(p, p') &= \hat{\Pi}_H^{\text{IR}}(p, p') + \int_\mu^\infty ds \hat{I}_\rho^{\text{mix}}(p, s) \hat{\Pi}_H^{\text{mix}}(s, p') \\ &+ \int_p^\mu ds \hat{I}_\rho^{\text{IR}}(p, s) \hat{\Pi}_H^{\text{IR}}(s, p'). \end{aligned} \quad (\text{F6})$$

The first and third terms on the right-hand side correspond to the IR contribution whereas the second term is

the contribution from high momentum modes. The former involves the functions  $\hat{\Pi}_H^{\text{IR}}$ , which itself receives contributions from high momentum modes, as we shall see shortly, and the latter involves the mix behaviors  $\hat{\Pi}_H^{\text{xim}}$  and  $\hat{I}_\rho^{\text{mix}}$ , which connect IR and UV modes. Applying a similar treatment to Eq. (45), we get, for the IR behavior ( $p, p' \ll 1$ ),

$$\begin{aligned} \hat{\Pi}_H^{\text{IR}}(p, p') &= \hat{\Pi}_F^{\text{IR}}(p, p') - \int_\mu^\infty ds \hat{\Pi}_F^{\text{mix}}(p, s) \hat{I}_\rho^{\text{xim}}(s, p') \\ &\quad - \int_{p'}^\mu ds \hat{\Pi}_F^{\text{IR}}(p, s) \hat{I}_\rho^{\text{IR}}(s, p') \end{aligned} \quad (\text{F7})$$

and, for the ‘‘xim’’ behavior ( $p' \lesssim \mu \lesssim p$ ),

$$\begin{aligned} \hat{\Pi}_H^{\text{xim}}(p, p') &= \hat{\Pi}_F^{\text{xim}}(p, p') - \int_\mu^\infty ds \hat{\Pi}_F^{\text{UV}}(p, s) \hat{I}_\rho^{\text{xim}}(s, p') \\ &\quad - \int_{p'}^\mu ds \hat{\Pi}_F^{\text{xim}}(p, s) \hat{I}_\rho^{\text{IR}}(s, p'). \end{aligned} \quad (\text{F8})$$

Here, the functions  $\hat{\Pi}_H^{\text{xim}}(p, p') = \hat{\Pi}_H^{\text{mix}}(p', p)$  and  $\hat{\Pi}_F^{\text{UV}}$  are known whereas the functions  $\hat{I}_\rho^{\text{IR}}$  and  $\hat{I}_\rho^{\text{xim}}$  are to be determined. Applying again the same technique as above to Eq. (43) we get, for the former (which involves  $p, p' \lesssim \mu$ )

$$\hat{I}_\rho^{\text{IR}}(p, p') = \hat{\Pi}_\rho^{\text{IR}}(p, p') + \int_p^{p'} ds \hat{\Pi}_\rho^{\text{IR}}(p, s) \hat{I}_\rho^{\text{IR}}(s, p'). \quad (\text{F9})$$

The solution of this equation is given in Eq. (65). Indeed, the integral in Eq. (43) for the  $\rho$  component only involves momenta  $s$  of the order of the external momenta  $p$  and  $p'$  and thus the IR behavior receives no contribution from UV modes.

For the function  $\hat{I}_\rho^{\text{xim}}$ , we use the relation  $\hat{I}_\rho^{\text{xim}}(p, p') = -\hat{I}_\rho^{\text{mix}}(p', p)$  and write (so, below,  $p \lesssim \mu \lesssim p'$ )

$$\hat{I}_\rho^{\text{mix}}(p, p') = \hat{\Pi}_{\rho, H}^{\text{mix}}(p, p') + \int_p^\mu ds \hat{\Pi}_\rho^{\text{IR}}(p, s) \hat{I}_\rho^{\text{mix}}(s, p'), \quad (\text{F10})$$

where we defined

$$\hat{\Pi}_{\rho, H}^{\text{mix}}(p, p') = \hat{\Pi}_\rho^{\text{mix}}(p, p') + \int_\mu^{p'} ds \hat{\Pi}_\rho^{\text{mix}}(p, s) \hat{I}_\rho^{\text{UV}}(s, p'). \quad (\text{F11})$$

These equations have a similar structure as those we solved when discussing  $\hat{I}_F^{\text{IR}}$ , i.e., Eqs. (44) and (45), with the upper bound replaced by  $\mu$ . We apply a similar technique as that used in Sec. V which exploits the fact that the function  $\hat{\Pi}_\rho^{\text{mix}}$  factorizes; see Eq. (F2). In particular, Eq. (F11) implies that the function  $\hat{\Pi}_{\rho, H}^{\text{mix}}$  can also be factorized:

$$\hat{\Pi}_{\rho, H}^{\text{mix}}(p, p') = A(p) \bar{B}_\rho(p'), \quad (\text{F12})$$

with

$$\bar{B}_\rho(p) = B_\rho(p) - \int_\mu^p ds \hat{I}_\rho^{\text{UV}}(p, s) B_\rho(s). \quad (\text{F13})$$

The function  $\hat{I}_\rho^{\text{UV}}$  is entirely determined by UV physics. It solves the following equation:

$$\hat{I}_\rho^{\text{UV}}(p, p') = \hat{\Pi}_\rho^{\text{UV}}(p, p') + \int_p^{p'} ds \hat{\Pi}_\rho^{\text{UV}}(p, s) \hat{I}_\rho^{\text{UV}}(s, p'), \quad (\text{F14})$$

which, for  $|\ln p/p'| = |t - t'| \ll 1$  reduces to the equation for resumming bubbles in the Minkowski vacuum; see Eqs. (E6) and (E7). We note, in particular, that this equation does not generate any infrared enhancement factor. Each new bubble generated by the integral equation thus brings a genuine coupling factor  $\lambda$ .

Now, using Eq. (F9), one shows that Eq. (F10) can be solved as, see Appendix A,

$$\hat{I}_\rho^{\text{mix}}(p, p') = \hat{\Pi}_{\rho, H}^{\text{mix}}(p, p') + \int_p^\mu ds \hat{I}_\rho^{\text{IR}}(p, s) \hat{\Pi}_{\rho, H}^{\text{mix}}(s, p'), \quad (\text{F15})$$

from which it follows that

$$\hat{I}_\rho^{\text{mix}}(p, p') = \bar{A}(p) \bar{B}_\rho(p'), \quad (\text{F16})$$

with

$$\bar{A}(p) = A(p) + \int_p^\mu ds \hat{I}_\rho^{\text{IR}}(p, s) A(s). \quad (\text{F17})$$

We note that Eq. (F17) is identical to Eq. (69) which we solved in Sec. V. We thus have

$$\bar{A}(p) = i \sqrt{\frac{-\pi_F}{p}} \bar{\mathcal{A}} \left( \ln \frac{p}{\mu} \right) = \frac{i \sqrt{-\pi_F}}{p^{\bar{\kappa} + \frac{1}{2}}}, \quad (\text{F18})$$

with  $\bar{\kappa} = \bar{\nu} - \varepsilon$ .

Inserting  $\hat{I}_\rho^{\text{xim}}(p, p') = -\hat{I}_\rho^{\text{mix}}(p', p) = -\bar{B}_\rho(p) \bar{A}(p')$  in (F7), we obtain

$$\hat{\Pi}_H^{\text{IR}}(p, p') = A(p) \bar{A}(p') \left\{ 1 + \int_\mu^\infty ds \bar{B}_\rho(s) B_F(s) \right\}, \quad (\text{F19})$$

where we used the factorization property (F1) as well as Eq. (F17). Similarly, we get, from (F8),

$$\hat{\Pi}_H^{\text{xim}}(p, p') = \left\{ B_F(p) + \int_\mu^\infty ds \hat{\Pi}_F^{\text{UV}}(p, s) \bar{B}_\rho(s) \right\} \bar{A}(p'). \quad (\text{F20})$$

We emphasize that the integrals in both (F19) and (F20) are finite in  $d = 3$  as can be checked from Eqs. (E6), (F4), (F5) and (F13). All the ingredients entering the right-hand side of Eq. (F6) have now been determined. Using again Eq. (F9), we finally obtain

$$\hat{I}_F^{\text{IR}}(p, p') = Z \bar{A}(p) \bar{A}(p'), \quad (\text{F21})$$

with the renormalization factor

$$\begin{aligned} Z &= 1 + 2 \int_\mu^\infty ds \bar{B}_\rho(s) B_F(s) \\ &\quad + \int_\mu^\infty ds ds' \bar{B}_\rho(s) \hat{\Pi}_F^{\text{UV}}(s, s') \bar{B}_\rho(s'). \end{aligned} \quad (\text{F22})$$

It is remarkable that Eq. (F21), which fully takes into account UV modes, is essentially identical to the solution obtained in Sec. V, see Eqs. (71) and (75), where UV modes were neglected. Superhorizon modes only affect the final result through a constant, finite renormalization factor  $Z$ . This important result shows that there is an effective decoupling of UV and IR physics in de Sitter space.

The fact that the statistical two-point function  $\hat{I}_F$  (the two-point statistical function of the composite operator  $\varphi^2$ ) takes a factorized form, Eq. (F21), in the IR is a remarkable result too. As already emphasized in Sec. V, this is reminiscent of the fact that de Sitter IR fluctuations can be described by a classical stochastic ensemble of growing modes [57–59]. Here, we emphasize another interesting result, namely the fact that the spectral component  $\hat{I}_\rho$  also factorizes in the mix regime, see Eq. (F16). This is also rooted in the classical statistical nature of IR fluctuations in de Sitter and is to be put in parallel with the corresponding factorized form of the spectral function of the field  $\varphi$ , Eq. (B12).

We end this section with a few remarks concerning the renormalization factor (F22). The parametric dependence of the various factors in (F22) on the coupling constant  $\lambda$  is as follows. From Eqs. (E6) and (F14) we get  $\hat{\Pi}^{UV} \sim \lambda$  and  $\hat{I}^{UV} \sim \lambda(1 + \mathcal{O}(\lambda))$ . This implies that  $\bar{B}_\rho \sim B_\rho(1 + \mathcal{O}(\lambda))$ , see Eq. (F13). Recalling that  $B_{F,\rho} \sim \sqrt{\pi_\rho}$ , where  $\pi_\rho \sim \lambda/\varepsilon$ , Eqs. (F4) and (F5), we thus have

$$Z - 1 \sim \pi_\rho(1 + \mathcal{O}(\lambda)). \quad (\text{F23})$$

As discussed in Sec. VI, one has either  $\pi_\rho \sim \sqrt{\lambda}$ , in the case of a vanishing tree-level square mass, or  $\pi_\rho \sim 1$  in the case of negative tree-level square mass. In any case, for small coupling we can approximate  $\bar{B}_{F,\rho} \approx B_{F,\rho}$  and write, using (F4) and (F5),

$$\begin{aligned} Z &\approx 1 - 2\pi_F \int_\mu^\infty ds \frac{\sin 2s}{s^2} \\ &\approx 1 + 2\pi_\rho \left\{ \frac{\sin 2\mu}{2\mu} - \text{Ci}(2\mu) \right\}, \end{aligned} \quad (\text{F24})$$

where we used  $\pi_F = -\pi_\rho F_\nu \approx -\pi_\rho/2$  in  $d = 3$ .

### Appendix G: Renormalization

The present theory is perturbatively renormalizable in  $D = d + 1 = 4$ . The renormalization of the gap equation (19) has been discussed in [33]. The main result is that it can be made finite by a standard (Minkowski-like, i.e., curvature independent) redefinition of the parameters  $m^2$ ,  $\xi$  and  $\lambda$ . Here, we discuss (for the first time to our knowledge in the present context) the renormalization of the four-point function Eq. (20), or (31).

As in previous sections, we regularize the theory by a simple sharp cutoff on physical momenta, i.e. by using the regularized propagator  $\hat{G}(p, p') \rightarrow \hat{G}(p, p')\theta(\Lambda -$

$p)\theta(\Lambda - p')$ . Such a cutoff on physical momenta actually breaks the de Sitter symmetry but is compatible with the  $p$ -representation, i.e., it does not break the affine subgroup of the de Sitter group, which is at the root of the  $p$ -representation [47]. Moreover, the local Lorentz—and thus de Sitter—symmetry is restored after renormalization provided one imposes suitable, i.e., covariant renormalization conditions. An alternative would be to employ de Sitter invariant regulators, such as dimensional [4, 6, 10], or Pauli-Villars [67] regularizations.

When discussing renormalization, i.e., the removal of the regulator, the decomposition (40) should be modified to take into account a local term

$$\hat{\Pi}(p, p') = i\hat{\pi}\delta_\varepsilon(p-p') + \hat{\Pi}_F(p, p') - \frac{i}{2}\text{sign}_\varepsilon(p-p')\hat{\Pi}_\rho(p, p'), \quad (\text{G1})$$

where  $\hat{\pi}$  is a (divergent) constant. This expresses the fact that  $i\hat{\Pi}(p, p')$  is a one-loop contribution to the four-point function, see (31), and thus potentially contains a (divergent) contribution with the same structure as the tree-level (bare) coupling<sup>8</sup>  $\sim \delta_\varepsilon(p - p')$ ; see (37). Let us now give a general analysis of the divergent contribution.

We recall the expression with  $d = 3$  spatial dimensions

$$\hat{\Pi}(p, p') = -\frac{\lambda}{6} \int_{\mathbf{q}} \frac{\hat{G}(qp, qp')\hat{G}(rp, rp')}{qr}, \quad (\text{G2})$$

with  $r = |\mathbf{e} + \mathbf{q}|$ . The divergent contribution  $\hat{\Pi}^{\text{div}}$  comes from very high momentum modes  $1 \ll \mu_r < qp, qp' < \Lambda$ , where  $\mu_r$  is an arbitrary (renormalization) scale. Specializing to the case  $p, p' \in \hat{C}^+$  for simplicity,<sup>9</sup> we thus have<sup>10</sup>

$$\hat{\Pi}^{\text{div}}(p, p') = -\frac{\lambda}{6} \int_{\tilde{\mu}_r < |\mathbf{q}| < \tilde{\Lambda}} \frac{\hat{G}_{\text{UV}}^2(qp, qp')}{q^2} \quad (\text{G3})$$

$$= -\frac{\lambda}{48\pi^2} \int_{\tilde{\mu}_r}^{\tilde{\Lambda}} dq e^{-2iq|p-p'|} \quad (\text{G4})$$

$$= \frac{\lambda}{96\pi^2} \frac{e^{-2i\tilde{\Lambda}|p-p'|} - e^{-2i\tilde{\mu}_r|p-p'|}}{i|p-p'|}, \quad (\text{G5})$$

where  $\tilde{\Lambda} \equiv \Lambda/\max(p, p')$  and  $\tilde{\mu}_r \equiv \mu_r/\max(p, p')$ . This expression agrees with our previous findings Eqs. (C18) and (E6).

To extract the divergent contribution in the limit  $\Lambda \rightarrow \infty$ , we use the well-known result

$$\frac{\sin 2\tilde{\Lambda}|x|}{|x|} \rightarrow \pi\delta(x) \quad (\text{G6})$$

<sup>8</sup> Equivalently,  $i\hat{\Pi}(p, p')$  is the one-loop contribution to the two-point correlator of the composite field  $\varphi^2$ , whose tree-level contribution is  $\sim \delta_\varepsilon(p - p')$ ; see (37).

<sup>9</sup> The general result has the same structure with the replacement  $|p - p'| \rightarrow -(p - p')\text{sign}_\varepsilon(p - p')$ .

<sup>10</sup> Note that it is sufficient to approximate  $r \approx q$  in order to get the leading (logarithmic) divergent behavior.



as well as

$$\frac{\cos 2\tilde{\Lambda}|x|}{|x|} \rightarrow 2 \ln \frac{\mu_r}{\Lambda} \delta(x) + \frac{\cos 2\tilde{\mu}_r|x|}{|x|}. \quad (\text{G7})$$

The latter can be shown as follows. For any test function  $f(x)$ , one has

$$\int dx f(x) \frac{\cos 2\tilde{\Lambda}|x| - \cos 2\tilde{\mu}_r|x|}{|x|} \rightarrow 2f(0) \int_0^\infty dy \frac{\cos y - \cos \frac{\mu_r}{\Lambda}y}{y} \quad (\text{G8})$$

$$= 2f(0) \lim_{\eta \rightarrow 0} \left[ \text{Ci} \left( \frac{\mu_r \eta}{\Lambda} \right) - \text{Ci}(\eta) \right] \quad (\text{G9})$$

$$= 2f(0) \ln \frac{\mu_r}{\Lambda}, \quad (\text{G10})$$

where we used  $\tilde{\mu}_r/\tilde{\Lambda} = \mu_r/\Lambda$ . We made the change of variable  $y = 2\Lambda x$  and took the limit  $\Lambda/\mu_r \gg 1$  in the second line. The third line is obtained by noticing that, since the integrand vanishes at  $y = 0$ , one can safely replace  $\int_0^\infty dy = \lim_{\eta \rightarrow 0} \int_\eta^\infty$ . Finally, we used  $\text{Ci}(x) = -\int_x^\infty dt \cos t/t = \ln x + \gamma + \mathcal{O}(x^2)$  at small  $x$ . We thus get the desired divergent contribution as

$$\hat{\Pi}^{\text{div}}(p, p') \rightarrow \frac{i\lambda}{48\pi^2} \ln \frac{\Lambda}{\mu_r} \delta(p - p'). \quad (\text{G11})$$

We note that, since the UV divergent term is local, one can replace  $p - p' \rightarrow -p(t - t')$ . One recovers the usual Minkowski one-loop coupling divergence for  $\sqrt{pp'} \hat{\Pi}(p, p') \rightarrow \Pi_{\text{Mink}}(t - t', p)$ :

$$\Pi_{\text{Mink}}^{\text{div}}(t - t', p) \rightarrow \frac{i\lambda}{48\pi^2} \ln \frac{\Lambda}{\mu_r} \delta(t - t'). \quad (\text{G12})$$

This guarantees that the divergence (G11) can be absorbed by the usual Minkowski counterterm. Incidentally, this ensures that the local Lorentz—hence de Sitter—symmetry is properly restored in the usual way after the UV cutoff is removed.

We are now in a position to discuss the renormalization of the resummation equation (39). For this purpose, it is convenient to extract the explicit coupling dependence of each term. We define

$$\hat{\Pi}(p, p') = \lambda \pi(p, p'), \quad \hat{I}(p, p') = \lambda^{-1} \mathfrak{S}(p, p'), \quad (\text{G13})$$

such that  $\pi \sim \lambda^0$  and  $\mathfrak{S} \sim \lambda^2$ . Equation (39) thus reads

$$\mathfrak{S}(p, p') = \lambda^2 \pi(p, p') - i\lambda \int_{\hat{c}} ds \pi(p, s) \mathfrak{S}(s, p'). \quad (\text{G14})$$

We have, from the above discussion,

$$\pi(p, p') = i\pi_{\text{div}} \delta_{\hat{c}}(p - p') + \pi^f(p, p'), \quad (\text{G15})$$

where  $\pi^f(p, p')$  is finite and

$$\pi_{\text{div}} = -\frac{1}{48\pi^2} \ln \frac{\Lambda}{\mu_r}. \quad (\text{G16})$$

Accordingly, we write

$$\mathfrak{S}(p, p') = i\mathfrak{S}_{\text{div}} \delta_{\hat{c}}(p - p') + \mathfrak{S}^f(p, p'), \quad (\text{G17})$$

where  $\mathfrak{S}^f(p, p')$  is finite, as shown below. Plugging the expressions (G15) and (G17) in Eq. (G14), we get

$$\mathfrak{S}_{\text{div}} = \frac{\lambda^2 \pi_{\text{div}}}{1 - \lambda \pi_{\text{div}}} \quad (\text{G18})$$

and, after some simple manipulations,

$$\mathfrak{S}^f(p, p') = \lambda_r^2 \pi^f(p, p') - i\lambda_r \int_{\hat{c}} ds \pi^f(p, s) \mathfrak{S}^f(s, p'), \quad (\text{G19})$$

where we introduced the renormalized coupling

$$\lambda_r = \frac{\lambda}{1 - \lambda \pi_{\text{div}}} = \frac{\lambda}{1 + \frac{\lambda}{48\pi^2} \ln \frac{\Lambda}{\mu_r}}. \quad (\text{G20})$$

This is the standard expression for the renormalized coupling in the large- $N$  limit, up to possible (renormalization-scheme-dependent) finite parts [27]. It shows the trivial character of the present theory, i.e., that for any positive bare coupling  $\lambda$ , the running coupling  $\lambda_r \rightarrow 0^+$  in the IR, i.e., for  $\mu_r/\Lambda \rightarrow 0$ . Reversely, demanding that  $\lambda_r$  be finite, Eq. (G20) expresses how the bare coupling  $\lambda$  evolves as the cutoff is removed:  $1/\lambda = 1/\lambda_r + \pi_{\text{div}}$ . One gets the usual Landau pole in the UV, the value  $\Lambda_L$  of the cutoff where the bare coupling diverges:  $\Lambda_L/\mu_r = \exp(48\pi^2/\lambda_r)$ . Finally, we stress that the renormalized coupling (G20) coincides with that needed to absorb coupling subdivergences in the equation for self-energy  $\Sigma$  [33], as expected.

Using the large momentum behavior of the  $F$  and  $\rho$  components of the function  $\pi^f(p, s \rightarrow \infty)$ , which can be inferred from the previous sections, see Eqs. (D34), (D35) and (E6), one can show that the contour integral in (G19) does not lead to UV divergence. This is related to the fact that this is originally a time integral, and not a momentum loop integral. Thus, we conclude that the function  $\mathfrak{S}^f(p, p')$  is finite when expressed in terms of the renormalized coupling  $\lambda_r$ . To make link with the original functions  $\hat{\Pi}$  and  $\hat{I}$  discussed in the paper, we define the finite functions

$$\hat{\Pi}^r(p, p') = \lambda_r \pi^f(p, p'), \quad \hat{I}^r(p, p') = \lambda_r^{-1} \mathfrak{S}^f(p, p'), \quad (\text{G21})$$

in terms of which Eq. (G19) reads

$$\hat{I}^r(p, p') = \hat{\Pi}^r(p, p') - i \int_{\hat{c}} ds \hat{\Pi}^r(p, s) \hat{I}^r(s, p'). \quad (\text{G22})$$

This is to be compared to Eq. (39). This shows that the discussion presented in the main body of the paper (including appendices) readily applies to the renormalized quantities defined here provided one replaces bare quantities  $\lambda$ ,  $\hat{\Pi}$ , and  $\hat{I}$  by their renormalized counterparts  $\lambda_r$ ,  $\hat{\Pi}^r$ , and  $\hat{I}^r$ , together with the replacement  $\Lambda \rightarrow \mu_r$  in momentum loop integrals.

To close this section, we note that the bare function  $\hat{I}(p, p')$  is not finite, but contains a local divergence  $\sim i\lambda_r\pi_{\text{div}}\delta_{\hat{c}}(p - p')$ , see Eqs. (G13),(G17), and (G18). This is, however, not a problem since  $\hat{I}$  is not directly a physical quantity but merely the loop correction to either the two-point correlator  $\hat{D}$ , see Eq. (37), or, equivalently, the four-point vertex function, see Eq. (20), or (31). One easily checks that these physical quantities are finite after renormalization. Using Eqs. (G13),(G17), (G18), (G20),

and (G22), one finds that

$$\begin{aligned} i\hat{D}(p, p') &= -\frac{\lambda}{3N} \left[ -\delta_{\hat{c}}(p - p') + i\hat{I}(p, p') \right] \\ &= -\frac{\lambda_r}{3N} \left[ -\delta_{\hat{c}}(p - p') + i\hat{I}^r(p, p') \right] \end{aligned} \quad (\text{G23})$$

is finite and thus so is the four-point vertex function (31).

- 
- [1] N. C. Tsamis and R. P. Woodard, Phys. Rev. D **54** (1996) 2621.
- [2] T. Prokopec, O. Tornkvist and R. P. Woodard, Phys. Rev. Lett. **89** (2002) 101301.
- [3] T. Brunier, V. K. Onemli and R. P. Woodard, Class. Quant. Grav. **22**, 59 (2005).
- [4] S. Weinberg, Phys. Rev. D **72** (2005) 043514; Phys. Rev. D **74** (2006) 023508.
- [5] M. S. Sloth, Nucl. Phys. B **748** (2006) 149. Nucl. Phys. B **775** (2007) 78.
- [6] D. Seery, JCAP **0711** (2007) 025; JCAP **0802** (2008) 006.
- [7] M. van der Meulen and J. Smit, JCAP **0711** (2007) 023.
- [8] G. Geshnizjani and R. Brandenberger, Phys. Rev. D **66** (2002) 123507.
- [9] Y. Urakawa and T. Tanaka, Prog. Theor. Phys. **122** (2009) 779; Phys. Rev. D **82** (2010) 121301.
- [10] L. Senatore and M. Zaldarriaga, JHEP **1012** (2010) 008.
- [11] E. O. Kahya, V. K. Onemli and R. P. Woodard, Phys. Lett. B **694**, 101 (2010).
- [12] A. A. Starobinsky and J. Yokoyama, Phys. Rev. D **50** (1994) 6357.
- [13] V. K. Onemli and R. P. Woodard, Class. Quant. Grav. **19**, 4607 (2002); Phys. Rev. D **70**, 107301 (2004)
- [14] N. C. Tsamis and R. P. Woodard, Nucl. Phys. B **724** (2005) 295.
- [15] C. P. Burgess, L. Leblond, R. Holman and S. Shandera, JCAP **1003** (2010) 033; JCAP **1010** (2010) 017.
- [16] L. H. Ford, Phys. Rev. D **31** (1985) 710.
- [17] E. Mottola, Phys. Rev. D **33** (1986) 1616;
- [18] I. Antoniadis, J. Iliopoulos and T. N. Tomaras, Phys. Rev. Lett. **56** (1986) 1319.
- [19] N. C. Tsamis and R. P. Woodard, Nucl. Phys. B **474** (1996) 235.
- [20] A. M. Polyakov, Nucl. Phys. B **834** (2010) 316.
- [21] D. Marolf and I. A. Morrison, Phys. Rev. D **84** (2011) 044040.
- [22] S. Hollands, arXiv:1010.5367 [gr-qc]; Annales Henri Poincare **13** (2012) 1039.
- [23] S. Weinberg, in *Conceptual foundations of quantum field theory*, edited by T.Y. Cao. (Cambridge University Press, Cambridge, England 1999), pp. 241-251.
- [24] B. Delamotte, Lect. Notes Phys. **852** (2012) 49.
- [25] J. -P. Blaizot, E. Iancu and A. Rebhan, in *Quark Gluon Plasma*, edited by R.C. Hwa *et al.* pp. 60-122.
- [26] J. Berges and J. Serreau, hep-ph/0302210; hep-ph/0410330; J. Berges, AIP Conf. Proc. **739**, 3 (2005).
- [27] S. R. Coleman, R. Jackiw and H. D. Politzer, Phys. Rev. D **10** (1974) 2491.
- [28] R. G. Root, Phys. Rev. D **10** (1974) 3322.
- [29] D. Boyanovsky, H. J. de Vega, R. Holman and M. Simionato, Phys. Rev. D **60** (1999) 065003.
- [30] J. M. Cornwall, R. Jackiw and E. Tomboulis, Phys. Rev. D **10** (1974) 2428.
- [31] A. Riotto and M. S. Sloth, JCAP **0804** (2008) 030.
- [32] B. Garbrecht and G. Rigopoulos, Phys. Rev. D **84** (2011) 063516.
- [33] J. Serreau, Phys. Rev. Lett. **107** (2011) 191103.
- [34] T. Prokopec, JCAP **1212** (2012) 023.
- [35] T. Arai, Class. Quant. Grav. **29** (2012) 215014; Phys. Rev. D **86** (2012) 104064.
- [36] D. Boyanovsky, Phys. Rev. D **85** (2012) 123525; Phys. Rev. D **86** (2012) 023509.
- [37] A. Rajaraman, Phys. Rev. D **82** (2010) 123522.
- [38] M. Beneke and P. Moch, arXiv:1212.3058 [Phys. Rev. D (to be published)].
- [39] R. Parentani and J. Serreau, Phys. Rev. D **87**, 045020 (2013).
- [40] E. T. Akhmedov, JHEP **1201**, 066 (2012); E. T. Akhmedov and P. Burda, Phys. Rev. D **86**, 044031 (2012); E. T. Akhmedov, F. K. Popov and V. M. Slepukhin, arXiv:1303.1068 [hep-th].
- [41] A. Youssef and D. Kreimer, arXiv:1301.3205 [gr-qc].
- [42] F. Cooper, S. Habib, Y. Kluger, E. Mottola, J. P. Paz and P. R. Anderson, Phys. Rev. D **50** (1994) 2848.
- [43] J. Berges, Nucl. Phys. A **699** (2002) 847; G. Aarts, D. Ahrensmeier, R. Baier, J. Berges and J. Serreau, Phys. Rev. D **66** (2002) 045008.
- [44] J. Baacke and S. Michalski, Phys. Rev. D **70** (2004) 085002.
- [45] B. Ratra, Phys. Rev. D **31** (1985) 1931.
- [46] N. D. Mermin and H. Wagner, Phys. Rev. Lett. **17** (1966) 1133.
- [47] X. Busch and R. Parentani, Phys. Rev. D **86** (2012) 104033.
- [48] J. Adamek, X. Busch and R. Parentani, arXiv:1301.3011 [hep-th].
- [49] J. S. Schwinger, J. Math. Phys. **2** (1961) 407;
- [50] P. M. Bakshi and K. T. Mahanthappa, J. Math. Phys. **4** (1963) 1; *ibid* **12**;
- [51] L. V. Keldysh, Zh. Eksp. Teor. Fiz. **47** (1964) 1515 [Sov. Phys. JETP **20** (1965) 1018].
- [52] K. -c. Chou, Z. -b. Su, B. -l. Hao and L. Yu, Phys. Rept. **118** (1985) 1;
- [53] S. A. Ramsey and B. L. Hu, Phys. Rev. D **56** (1997) 661.
- [54] A. Tranberg, JHEP **0811** (2008) 037.
- [55] T. S. Bunch and P. C. W. Davies, Proc. Roy. Soc. Lond. A **360** (1978) 117.
- [56] I. S. Gradshteyn, I. M. Ryzhik, *Table of Integrals, Series*

*and Products*, Academic Press, N.Y., 1980.

- [57] A. H. Guth and S. -Y. Pi, Phys. Rev. D **32** (1985) 1899.
- [58] D. Polarski and A. A. Starobinsky, Class. Quant. Grav. **13** (1996) 377.
- [59] D. Campo and R. Parentani, Phys. Rev. D **70** (2004) 105020.
- [60] A. Coutant, A. Fabbri, R. Parentani, R. Balbinot and P. Anderson, Phys. Rev. D **86** (2012) 064022; A. Coutant and R. Parentani, arXiv:1211.2001 [physics.flu-dyn].
- [61] Y. Korai and T. Tanaka, Phys. Rev. D **87** (2013) 024013.
- [62] D. P. Jatkar, L. Leblond and A. Rajaraman, Phys. Rev. D **85** (2012) 024047.
- [63] F. Gautier and J. Serreau, work in progress.
- [64] D. Campo and R. Parentani, Phys. Rev. D **72** (2005) 045015; Phys. Rev. D **78** (2008) 065044.
- [65] P. C. Martin, E. D. Siggia and H. A. Rose, Phys. Rev. A **8** (1973) 423.
- [66] G. Aarts and J. Smit, Nucl. Phys. B **511** (1998) 451; G. Aarts and J. Berges, Phys. Rev. Lett. **88** (2002) 041603.
- [67] S. Weinberg, Phys. Rev. D **83** (2011) 063508.